

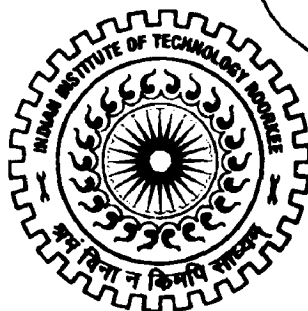
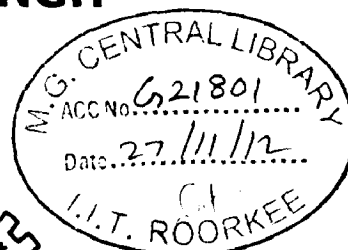
# SYNTHESIS OF MESOPOROUS TITANIUM DIOXIDE FILMS FOR DYE-SENSITIZED SOLAR CELLS

## A DISSERTATION

*Submitted in partial fulfillment of the  
requirements for the award of the degree*  
of  
**MASTER OF TECHNOLOGY**  
in  
**NANOTECHNOLOGY**

By

**HARJEET SINGH**



**CENTER OF NANOTECHNOLOGY  
INDIAN INSTITUTE OF TECHNOLOGY ROORKEE  
ROORKEE -247 667 (INDIA)  
JUNE, 2012**



## CANDIDATE'S DECLARATION

I hereby declare that the work which is being presented in this report entitled "Synthesis of Mesoporous Titanium dioxide Films for Dye-Sensitized Solar Cells" submitted for the partial fulfillment of the degree of Master of Technology in Nanotechnology, submitted in the Centre of Nanotechnology, Indian Institute of Technology Roorkee, Roorkee is an authentic record of my own work carried out under the guidance of Dr.B.S.S.Daniel, Associate Professor, Department of Metallurgical and Materials Engineering, Indian Institute of Technology Roorkee, Roorkee.

Date: 14 June 2012  
Place: Roorkee

Harjeet Singh  
Enrollment No.- 10551007  
M.Tech. (2<sup>nd</sup> Year)  
Centre of Nanotechnology  
Indian Institute of Technology  
Roorkee, Roorkee. 247 667

## CERTIFICATE

This is to certify that the above declaration made by the candidate is correct to the best of my knowledge and belief.

Date: 14/6/2012  
Place: Roorkee

Dr. B.S.S. Daniel  
Associate Professor,  
Department of Metallurgical  
and Materials Engineering,  
Indian Institute of  
Technology Roorkee-247 667

## ACKNOWLEDGEMENT


I wish to express my deep sense of gratitude and sincere thanks to my guide Dr.B.S.S.Daniel, Associate Professor, Department of Metallurgical and Material Engineering, Indian Institute of Technology Roorkee, for his meticulous guidance and perpetual inspiration in completion of this dissertation. Working under his guidance was a privilege and an excellent learning experience that I will cherish forever.

I am thankful to the staff of Institute Instrumentation Center and Centre of Nanotechnology for extending their support for use of testing facilities.

I am also grateful to all my classmates especially Kiran. P Shejale,S Uday kumar,Raja Naren , Krishna Rao,Dharamveer,Amit and friends Vikram Dave, Sunil Baveja ,Tarun Sharma and Himanshu, Umesh Bind,Manjot Singh who were actively involved in providing me vital support in day to activities whenever I needed.

I would like to express my gratitude to my mother for her blessings that always provided me a strong support and inner strength. I am thankful to all my sisters , my brother Baljinder Singh and brother –in- law Dr.Ranjodh Singh for providing inspiration and motivation for completion of this work.

Last but not the least I am thankful to my daughter and my wife for their love and cooperation in this endeavor.

  
14/6/2012  
Harjeet Singh.

## ABSTRACT

Porous solid films offering large specific surface area and well connected cavities have been researched extensively in the last decade, aiming to enhance photo-conversion efficiency in the dye-sensitised solar cells (DSSCs). Generally, the photo-conversion efficiency of DSSCs is very sensitive to surface morphology, crystallinity and porosity of the film which are in turn highly dependent upon fabrication protocol. Preservation of ordered mesoporous structure is essential for increasing surface area in the films and is reported to be highly sensitive to pre-curing temperature. TiO<sub>2</sub> films were synthesised using layer-by-layer deposition in combination with block-polymer templating. The pre-curing temperature was varied between 200-300° Celsius for fabricating different sets of films. Influence of varying the pre-curing temperature on morphology and interfaces of film layers was investigated using AFM, SEM, EDX and UV-VIS Spectrophotometer. Also, a modified method of pre-curing temperature was employed successfully, in order to attain firm adhesiveness of the film to the conducting glass substrate, even at lower pre-curing temperatures below 250°C. The films prepared by different pre-curing temperature protocols were incorporated into DSSCs for evaluating its influence on the photo-conversion efficiency of the cells.



# Chapter 1

## INTRODUCTION

---

*For successful technology, reality must take precedence over*

*public relation, for nature cannot be fooled – Richard Feynman*

The energy usage is increasing very rapidly all over the world whereas the conventional energy resources are depleting day- by- day. The resultant deepening energy crisis is therefore, making it mandatory to look for renewable energy resources. The solar energy is very promising, clean and inexhaustible renewable source of energy because the solar panels convert sunlight directly into electricity. Merely 1% of the solar radiation received on the earth surface, if converted to electricity can meet the energy requirement of the world.

Dye Sensitised Solar Cells (DSSCs) have been regarded as promising next generation photovoltaic devices because of their unique characteristics such as comparable conversion efficiency at low cost involving simpler fabrication techniques .In honour to its inventor Michael Gratzel the cell is also referred to as Gratzel Cell. He was conferred with Millennium Technology Award by Technology Academy Finland, in 2010. With the application of nanotechnology, dye sensitised solar cells have become a strong competitor to silicon based solar cell because of its low cost, high stability while offering varied and fine tuned material choices. [1]. The DSSCs are composed of a dye-adsorbed wide band gap nano-crystalline oxide film on transparent conducting substrate used as photo-electrode, a redox electrolyte and a metallic counter electrode. The dye molecules play an important role in generating photo-excited electrons, the wide band gap nano-crystalline film provides a pathway for photo-excited electrons to move from dye to transparent conducting substrate and the redox electrolyte delivers electrons from counter electrode to oxidized dye to regenerate

dye. The photovoltaic performance of these devices is influenced by many factors such as morphology, film structure, porosity and particle size of the nano-crystalline semiconductor used as photo-electrode, molar absorption coefficient, absorption wavelength of photo-sensitizer dye, type of electrolytes, solid–solid and/or solid–liquid interfaces and electron transportation and recombination rates occurring in the device.

Based on the recent advances in s, research and technology, the dye sensitized solar cell stands a fairly good chance of gaining commercial viability, in comparison to the conventional silicon based solar cell as evidenced from the table-1.1 given below.

**Table-1.1: Comparison of Conventional silicon based cell and Dye sensitized solar cell**

<b>PARAMETER</b>	<b>SILICON BASED CELL</b>	<b>DYE-SENSITIZED SOLAR CELL</b>
Cell Layer Thickness	Thick layer	Thin layer
Processing Technique	Expensive	Cheaper
Absorption of light	Better	Poor
Short Circuit Current density	35 ma/sq cm	20 ma/ sq cm
Performance in Low light	Cuts off output	Better differential kinetics
Protective glass cover	Needed	Not Needed
On higher temperature	Output reduces	Less affected
Photo-conversion Efficiency	Typical- 15%, lab- 25%	Typical- 6%, lab-15%

The need of thinner layers typically 2-4 microns in case of DSSCs makes the cell array lighter, easy for transportation and cuts down the material cost significantly. Silicon needs exclusive fabrication set-up for its extraction and turning it into wafers under ultra clean laboratory conditions thus making the overall process expensive. Whereas, the process involved in DSSC is simpler and more cost effective. DSSC performs better under low lighting conditions compared to the silicon cells, so it is more suitable for cold regions and enhances average daily output in winter season by having longer operating hours. The power output of silicon cell is more adversely affected with rise in cell temperature above 25 degree Celsius than that of DSSC, so making DSSC more suitable for hot regions also. Although the efficiency of DSSC is lower but the cost factor dominates and makes DSSC the technology of choice as the cost /kilowatt of power produced is better than the silicon cell, even at lower efficiency.

In 2010 Sony announced fabrication of modules with efficiency close to 10% and hence opportunity of commercialization of DSSC modules is attainable. Application examples of dye sensitized solar cells and modules are DSSC panels installed in Newcastle (Australia)– the first commercial DSSC module (<http://www.sta.com.au/index.htm>), indoor ornament of dye sensitized solar cells leaves (AISIN SEIKI CO.,LTD) , flexible DSSC-based solar module developed by Dyesol (<http://www.dyesol.com>), and jacket commercialized by G24i (<http://www.g24i.com>).

The thin film nano-morphology can dramatically influence the competence of solar cells by employing chemical additives during solution processing. Attempts are also underway to make use of natural dyes which have the potential to be viable alternative to rare and expensive organic sensitizers because of their low cost, easy availability, abundant sources and environment friendliness [2]. DSSCs have been subject of a large number of experimental investigations in the recent past. The use of nanoscale constructs has given a major boost to

the solar photon conversion. DSSCs separate the optical absorption and charge separation process by associating a sensitizer with a wide-bandgap semiconductor of nanocrystalline morphology. Extended junction and nanostructured photo conversion device provide the pathway for light absorption and charge collection. Advantages of nano- sized semiconductor structures and particles include increased carrier lifetimes arising from space quantization, enhanced redox potentials of photo generated holes and electron arising from increased effective bandgap.

Efforts are continually being undertaken to improve the performance of DSSC owing to their potential of becoming commercially viable alternative to grid supply and hence, the competitiveness of this technology in the world market.

Nanotechnology has indeed opened up an entirely new domain in the development of efficient and economical solar cells. The improvement in the solar cell performance has been achieved by extensive studies on the optimization of dye, semiconductor film and redox electrolyte [3-7].

The use of sintered mesoporous titanium dioxide ( $\text{TiO}_2$ ) was the breakthrough that established DSSC technology and raised the DSSC efficiency from 1% (for cells having a non-porous  $\text{TiO}_2$  surface) to 7%. Titanium dioxide thin film coatings have been extensively used in solar cells to act as N-type semiconductor due to donor like oxygen vacancies.

More research is currently being carried out to further elucidate the mechanism(s) that limit the efficiency and electrical output .The improvement in the solar cell performance has been achieved by extensive studies on the optimization of dye, semiconductor film and redox electrolyte The DSSCs based on ruthenium dye sensitized nano-crystalline  $\text{TiO}_2$  electrodes and liquid redox electrolytes have already reached power conversion efficiency in the range 9–11% . Long-range ordered mesoporous  $\text{TiO}_2$  film would be a more efficient structure for

the electron transport, since it has minimized amount of grain boundaries. Furthermore, electrolyte diffusion will be highly efficient, since the pore size is uniform and all the pores are regularly interconnected. Therefore, long-range ordered mesoporous TiO<sub>2</sub> film will be a potential candidate for the photo-anode of DSSC.

Titanium dioxide films have wide applications as they are non-toxic, stable over wide pH, and low cost material having proven applied potential. Titanium dioxide nanoparticles facilitates tuneable band gap, chemically stable in water and have slow electron cooling (>1ns) as compared to (1ps) in case of bulk material.

Mesoporous Titanium dioxide films are extensively used in DSSCs due to their high specific surface area, uniform morphology of pores, and excellent connectivity of pores, which aids in efficient charge carrier transport due to better electrolyte diffusion.

Self assembly methods using block co-polymers have been effectively employed successfully in synthesis of mesoporous titanium dioxide films for facilitating controlled nano-morphology to enhance the efficiency of Dye Sensitized Solar Cells.

There is still much room left for optimizing the sol-gel and polymer coating processes by systematically and narrowly changing the parameters such as solution viscosity, spin rate, and sintering process.

**2.1 Historical Perspective** - In 1839 A. E. Becquerel observed photoelectric effect in an electrode immersed in a conductive solution exposed to light [8]. In 1954 the first silicon solar cell was demonstrated at Bell Laboratories. The interest in organic semiconductors revived in the 1977, when A. J. Heeger, A. G. MacDiarmid and H. Shirakawa discovered conducting polymers [9].

The use of dye-sensitization in photovoltaics remained rather unsuccessful until a breakthrough in 1991. In the Laboratory of Photonics and Interfaces in Switzerland, Grätzel and his co-workers developed a solar cell by the successful combination of nanostructured electrodes and efficient charge injection dyes. This cell was hence termed the dye sensitized nanostructured solar cell [10]. It is now possible to completely depart from the classical solid state junction device by replacing the phase contacting the semiconductor by an electrolyte, thereby forming a DSSC. According to [11] conversion efficiency records of 8.12%, 10.10%, 10.40% and 9.90% were announced at Energy Research Centre of The Netherlands, École Polytechnique Fédérale de Lausanne, Sharp Corporation and Arakawa group, respectively for solar cells . Apparently, the use of high haze TiO<sub>2</sub> electrodes led to the highest efficiency till date, standing at 11.10% [12].

DSSC photo-electrochemical cells have been subjected of a large number of experimental investigations since then. It falls in between solid-state photovoltaics and classical regenerative photo-electrochemical cell. The use of nanoscale constructs has given a major boost to the solar photon conversion. DSSC separates the optical absorption and charge separation process by associating a sensitizer with a wide-bandgap semiconductor of

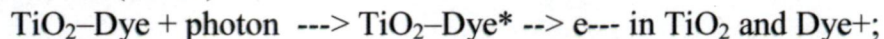
nanocrystalline morphology. Advantages of nanosized semiconductor structures and particles include increased carrier lifetimes arising from space quantization, enhanced redox potentials of photogenerated holes and electron arising from increased effective bandgap., Efforts are continually being undertaken to improve the performance of DSSC and hence the competitiveness of this technology in the world market.

## **2.2 DSSC operation**

DSSC parallels photosynthesis (figure 2.1), in the use of a dye as the light harvester to produce excited electrons,  $\text{TiO}_2$  replacing carbon dioxide as the electron acceptor, iodide/triiodide ( $\text{I}^-/\text{I}_3^-$ ) replacing water and oxygen as the electron donor and oxidation product and a multilayer structure to enhance both the light absorption and electron collection efficiency. The light-driven electrochemical process in DSSC is regenerative as shown in Fig. 2.2 and the working voltage produced by the device is the difference between the chemical potential of the  $\text{TiO}_2$  (Fermi level) and the redox potential of the mediator  $\text{I}^-/\text{I}_3^-$  [13]. Like photosynthesis, DSSC is a molecular machine that is one of the first devices to go beyond microelectronics into the realm of nanotechnology [14]. The latter process typically requires a catalytic amount of counter electrode, typically platinum (Pt) on the cathode surface. The process control is governed by kinetic competition.

The picture below shows the energetic of a finished blackberry---sensitized  $\text{TiO}_2$  solar cell and its operation under sunlight illumination. This process is more specifically described by the following equations:

On the  $\text{TiO}_2$  electrode (anode):



In the electrolyte solution:



On the graphite-coated counter electrode (cathode):  $\text{I}_3^- + 2 e^- \rightarrow 3 \text{I}^-;$

where  $\text{Dye}^*$  is the notation used when an electron has absorbed a photon

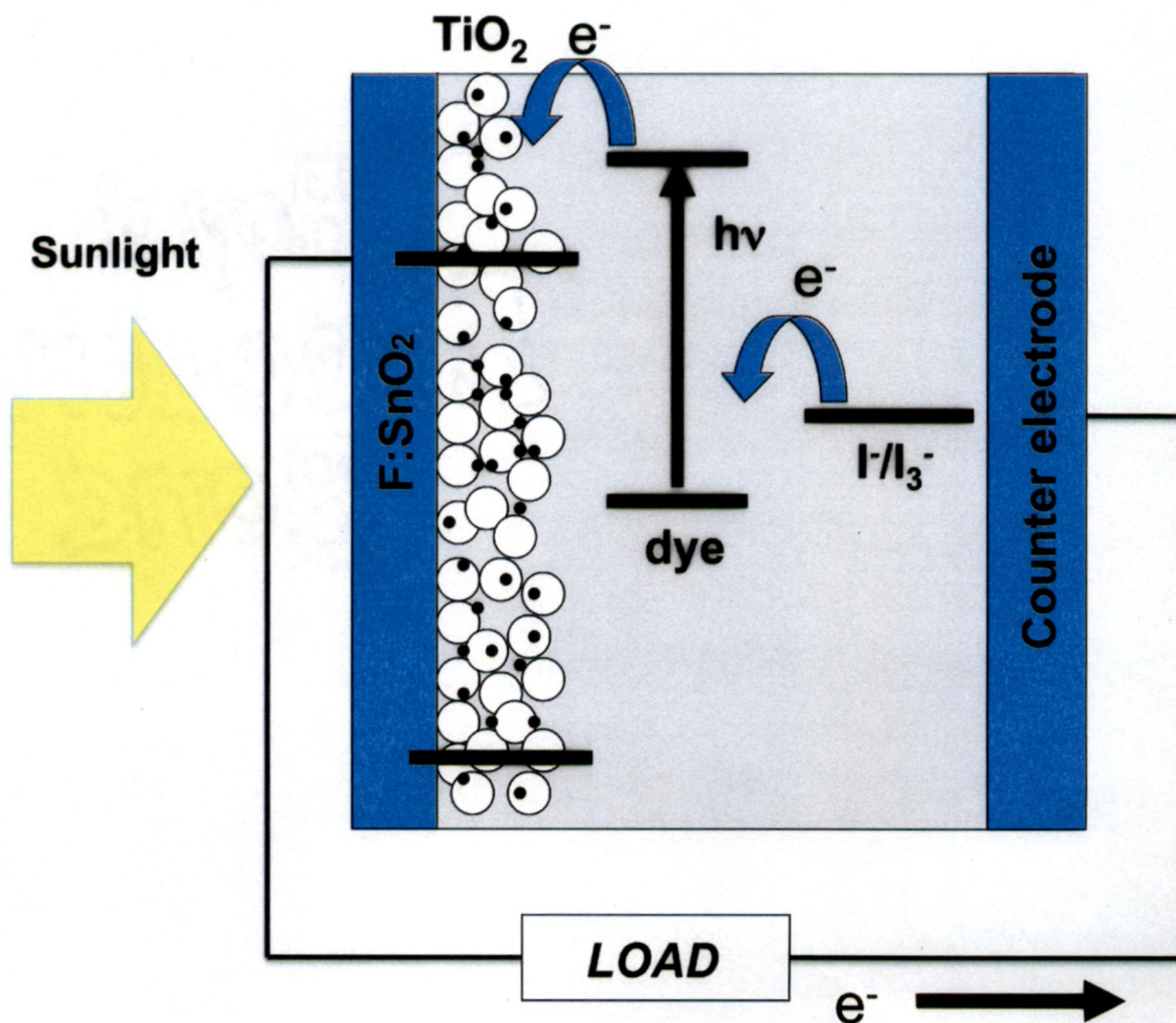


**Figure 2.1-** Schematic structure of DSSC. Upon light absorption, the dye is promoted into an electronically excited state from where it injects (within femtoseconds), an electron into the conduction band of a large bandgap semiconductor film ( $\text{TiO}_2$ ), onto which it is adsorbed. The electrons are transported through the  $\text{TiO}_2$  film by diffusion before reaching the anode of the cell. The positive charges resulting from the injection process are transferred into the liquid electrolyte by reaction of the dye cation, with the reduced species of a redox couple in the electrolyte solution. This leads to the generation of the charge neutral state of the sensitizer. The typical redox couple is  $\text{I}^-/\text{I}_3^-$ . After ionic diffusion, the carrier of the positive charge ( $\text{I}_3^-$ ) reaches the cathode, where it releases its charge thus being reduced back to  $\text{I}^-$ .



Although, the science is still far away from having a full understanding of the photosynthesis (Fig2.2) process, even a broad know-how of the process occurring at the nanoscale is astonishing.

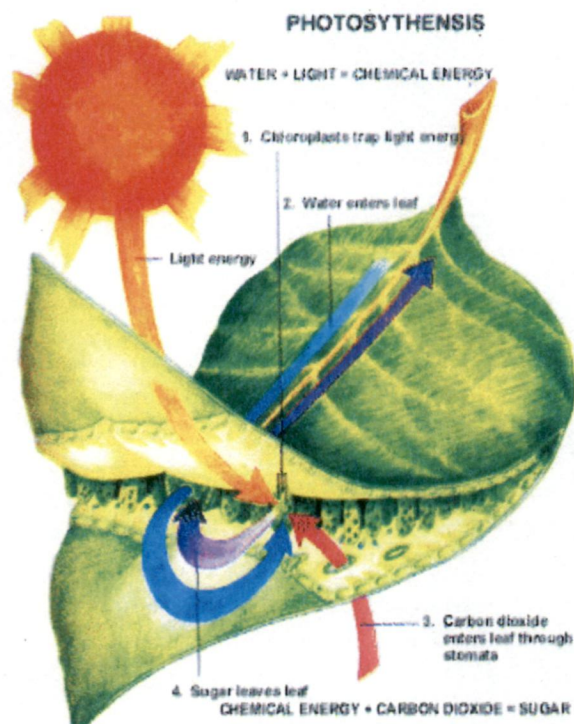


**Figure 2.2-Photosynthesis process in a plant leaf**

**Photosynthesis mechanism** -The sunlight is trapped by the chloroplasts, water is transported from soil to the leaf, carbon dioxide enters through stomata, water and light combines to form chemical energy, chemical energy and carbon dioxide rearrange to form carbohydrates, sugar is stored in plant and oxygen is released to the atmosphere.

Although the modern science is far away from mimicking the natural phenomenon but it does provide a great deal of inspiration for the designing of DSSCs.

### ***2.3 DSSC components***

DSSC converts visible light into electricity based on the sensitization of wide bandgap semiconductors and is primarily comprised of photo-electrode, redox electrolyte and counter electrode. Other materials include transparent conducting oxide and sealing agents. DSSC components have gone under various developments over the years in order to enhance the efficiency of the cell. 3.1. Titanium dioxide ( $\text{TiO}_2$ ) is the most popular electrode discussed for its' band gap, surface structure, particle size, porosity and film thickness in improving DSSC performance [15, 16]. However disadvantage of  $\text{TiO}_2$  is that electron mobility is too low, which is undesirable for higher conversion efficiency of solar cells [17, 18].

A solar cell works similarly to leaf of a plant. The chlorophyll dye (chlorophyll a) in a leaf, which was introduced in the biology lesson, absorbs solar energy and converts it into chemical energy (sugar); a solar cell takes solar energy and converts it into electrical energy, but creates no net chemical and thus is termed regenerative. Leaves store net chemical energy and are termed photosynthetic. Blackberries contain a strongly light--absorbing dye molecule called anthocyanin, which occurs in many types of fruits and berries. It is the compound that gives blackberries, raspberries, blueberries, and pomegranates their colour. These dyes can be extracted and used in a dye---sensitized  $\text{TiO}_2$  solar Cell to absorb light and convert the light's energy into electricity. Brian O'Regan and Michael Gratzel at the Ecole Polytechnique Federale De Lausanne in Switzerland made the first efficient DSSC. The Approach used in DSSCs has many advantages over other solar energy conversion technologies because of its simple device construction and inexpensive  $\text{TiO}_2$  particles and dyes that can be fine tuned to increase their light absorbing properties.

### ***2.4 Progress in mesoporous films***

Porous solids possessing large specific surfaces and easily accessible cavities have found wide applications in heterogeneous catalysis, sorption, separation, gas sensing, photo

electronics, host–guest chemistry, molecular electronic devices, medicine, and design of novel nanomaterials [19]. For the successful synthesis of mesoporous metal oxide films, precise control of the hydrolysis reaction of metal precursors to couple with the self-assembled surfactants is a prerequisite. Moreover, a proper surfactant with large ordering lengths is essential to achieve a robust mesoporous structure with extended thermal and mechanical stabilities.

For the last decade, the remarkable progress has been achieved in synthesis, characterization, and applications of highly organized mesoporous metal oxide films. Among the various metal oxides,  $\text{TiO}_2$  is of particular interest because of its unique physicochemical properties. Indeed, significant progress in mesoporous metal oxide films has been initiated by the successful preparation of  $\text{TiO}_2$  films in 2001, when Sanchez's, Kwon's, and Kuwabara's groups independently reported the synthesis of mesoporous  $\text{TiO}_2$  films in the anatase phase [20, 21]. Typically, a post-treatment step by aging the as-deposited films under humid atmosphere, as proposed by Sanchez and co-workers [22], permits the reproducible synthesis of high-quality mesoporous  $\text{TiO}_2$  nanocrystalline films with a long-range ordering. In 2002 and 2003, controllable synthesis of cubic mesoporous  $\text{TiO}_2$  films were reported by Stucky's and Sanchez's groups, respectively [23, 24]. Their synthetic strategies have been largely repeated by other scientists and have been a universal route to fabricate highly organized mesoporous  $\text{TiO}_2$  films with tuneable surface area, pore size and mesophase up to now.

### ***2.5 Mesoporous films applications***

Additionally, enhanced material properties originating from highly ordered mesoporous structures have been demonstrated in many applications, such as adsorption,

photocatalysis, catalyst supports, chromism, photovoltaic, luminescent devices, sensors, and others.

### ***2.6 Mesoporous TiO<sub>2</sub> film fabrication by Self-assembly of block copolymer***

In the sol-gel reaction, the diluted solution provides an excellent medium to sufficiently homogenize the block copolymer molecules and inorganic species at the atomic level as well as to retard inorganic polymerization. The cooperative liquid crystal template (CLCT) mechanism dominates the self-assembly between block copolymer and inorganic species in the solution. The partially hydrolyzed inorganic species with hydroxyl groups can cooperatively interact with hydrolytic regions of block copolymers through hydrogen bonding, forming a S<sub>0</sub>(I<sup>+</sup>X<sup>-</sup>)<sub>0</sub> interface [25], where S<sub>0</sub> is non-ionic surfactant, I<sup>+</sup> soluble cationic inorganic species, and X<sup>-</sup> soluble anions in solution.

After the homogeneous sol solution is coated on the heat resistant substrate, volatile components such as H<sub>2</sub>O, HCl, ethanol and other small-molecules or organic intermediates readily evaporate at the air/film interface. In contrast, the resident inorganic species and block copolymers are gradually concentrated, driving the phase segregation between the hydrophilic and hydrophobic blocks. Block copolymer-directing self-assembly energetically triggers the concentration of block copolymer in film to exceed the critical micelle concentration (CMC). Apparently, true liquid crystal liquid template (TLCT) mechanism is in operation at this stage, leading to the formation of various mesostructures. In-situ small-angle X-ray scattering (SAXS) coupled with interferometry analysis have indicated that the hybrid mesostructures are formed through the serial disorder-to-order transitions, from an isotropic sol to a worm-like mesophase, and to a highly organized mesostructure [26, 27].

### ***2.7 Thermal treatment***

Long-range ordered mesoporous structures can be generated by calcinations of the pre-organized mesoporous hybrid films in static air at an elevated temperature ( $\geq 300$  °C) at a

slow ramping rate (generally 1 °C/min). Additionally, Schouten's group [28] found that a low residual pressure (ca. 10 mbar) would be beneficial to preserving the mesoporous structure.

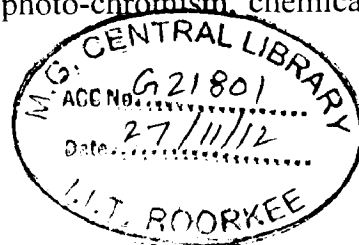
In general, the calcination temperature to achieve fully crystallized anatase phase is 450–500 °C. Thus, with calcination at 300–450 °C, the inorganic walls consist of mixture of amorphous TiO<sub>2</sub> and the anatase phase. Actually, the main shrinkage of mesoporous structure and the polyoriented crystal growth of the anatase grains occur at this temperature range. Interestingly, many reports have demonstrated that the rutile crystal phase is absent in the mesoporous TiO<sub>2</sub> films, even though they are calcined at 600–800 °C [29, 30].

Calcination temperature for highly organized mesoporous TiO<sub>2</sub> films should be optimized, since it strongly influences the textural property and thereby the photo-catalytic activity [31]. With increase of calcination temperature, mesoporous TiO<sub>2</sub> frameworks gradually crystallize and shrink, leading to decrease in the surface area while increase in crystallinity, crystal size, and pore diameter [32, 33]. Thus, the calcination temperature has to be adjusted to balance these parameters in order to achieve a highest photo-catalytic activity. Ozin's [34], Yu's [35], and Sanchez's [36] groups found that the films calcined at 400, 500 and 600 °C showed the highest photo-catalytic activity, respectively. The difference in calcinations temperature may be due to the difference in synthesis condition of mesoporous TiO<sub>2</sub> films and kinds of photo-catalytic reactions.

## ***2.8 Photocatalytic performances of mesoporous TiO<sub>2</sub> films***

Despite their low crystallinity, mesoporous TiO<sub>2</sub> films have demonstrated remarkably high photo-catalytic activities than the nonporous films in water splitting [37] and in complete degradation of organic contaminations, such as organic dyes [38, 39], stearic acid [40], and lauric acid [41] in aqueous media, or gaseous pollutants such as acetone [42] and 2-propanol [43, 44]. Excellent water disinfection property of mesoporous TiO<sub>2</sub> films was also found in killing *Escherichia coli*; a representative bacterium widely exists in the aquatic environment

[45]. The superior performances of mesoporous TiO<sub>2</sub> films in various photo-catalytic reactions are mainly attributed to their large accessible surface area and well-defined mesopores with uniform pore size and excellent connectivity, in which both effective charge carrier transfer and efficient mass flow of the reactants and products can be easily achieved. Highly organized mesoporous polymer films may be promising candidates as hard templates for the creation of mesoporous structure for TiO<sub>2</sub> films. Due to their well-defined mesopore-wall structure for fast charge carrier transport and large surface area for more molecular adsorption, highly organized mesoporous TiO<sub>2</sub> films with enhanced photochemical and electrochemical properties offer great opportunities in applications such as photo-catalysis, DSSC, catalytic chemical synthesis, energy storage, drug delivery and others. Considerable challenges still remain in developing high-quality mesoporous TiO<sub>2</sub> films with a thickness up to several micrometers in order to realize the practical applications in photo-electronic devices. The mesoporous structure is easily collapsed once the thickness of the mesoporous TiO<sub>2</sub> films reaches a critical dimension. Besides, the package density of most currently developed mesoporous TiO<sub>2</sub> films is quite low as compared to that of mesoporous TiO<sub>2</sub> spheres consisting of close-packed nano-crystallines [46]. As a result, the dye adsorption and photovoltaic conversion efficiency are seriously limited. Effects of the textural parameters in mesoporous TiO<sub>2</sub> films, especially wall thickness, pore-size, and pore volume, on the performances of the fabricated devices of DSSC should be well established. Research also should focus on the mesoporous multi-component TiO<sub>2</sub>-based films. Undoubtedly, mesoporous metal/ TiO<sub>2</sub> films attracted most interest due to their multifunctional properties enabling many potential applications. Conductive metal nanoparticles confined in mesoporous TiO<sub>2</sub> matrix possessing surface Plasmon resonance (SPR) characteristics or high catalytic activities lead to important applications such as photo-chromism, chemical synthesis, photo-catalysis, advanced materials design and others.



In order to realize thicker films, multilayered TiO<sub>2</sub> films were prepared using doctor-blade or layer-by-layer deposition methods [47, 48]. Among these two methods, the mesostructure formed by doctor-blade method lacked a long-range ordering, and the TiO<sub>2</sub> nanoparticles in the film were randomly interconnected forming an irregular inorganic framework [49], whereas the film prepared through layer-by-layer deposition showed a highly ordered cubical mesoporous structure [50]. DSSC conversion efficiencies up to 5.35% were then reported.

Highly crystallized and ordered mesoporous TiO<sub>2</sub> films with sufficient thickness up to few micrometers were successfully prepared via a supramolecular-templated sol-gel route and layer-by-layer deposition. The multilayered TiO<sub>2</sub> films as photo-anodes were integrated into the DSSCs. Firstly, the DSSC performance showed a strong dependence on the film thickness. For the film pre-cured at 350 °C, the energy conversion efficiency rises with increasing film thickness initially and then declines when the thickness is above 2.20 μm. A maximum efficiency (4.04%) was achieved for the film of 2.20 μm thickness. Secondly, the pre-curing temperature is an important parameter for achieving a high photovoltaic performance. Any uncontrolled crystallization at relatively high pre-curing temperature leads to contraction or even collapse of mesopores and thus loss of surface area. Too low a temperature (200 °C) leads to a loose attachment of the film to the substrate. A maximum efficiency of 5.1% was successfully achieved for the film of 2.20 μm thick that was pre-cured at 250 °C [51].

The efficiency of DSSCs highly depends upon the particle size of TiO<sub>2</sub>, surface morphology, and porosity of the film. At lower temperatures mesopores are preserved so short circuit current (I<sub>sc</sub>) goes up but poor adhesion to substrate reduces electron transport on interface and efficiency falls dramatically. At higher temperatures mesopores collapse reducing the surface area, decreasing efficiency.

Recent reports have presented a correlation between the thickness of the TiO<sub>2</sub> film and its surface roughness Zaharescu et al. presented results suggesting a relationship between the processing temperature and surface topography of TiO<sub>2</sub> films.[53]

### ***2.81 Advancements and challenges***

Development of a facile and general methodology for the synthesis of highly organized mesoporous metal oxides encounters many challenges, such as:

(1) Chemical diversity of metal oxides as well as the availability of an appropriate precursor (a synthetic approach to creating a mesoporous metal oxide often strongly depends upon the nature of the metal precursor and targeted metal oxide.);

(2) Difficulty in controlling the reactivity of metal precursors (different from Si sources, transition metal precursors are highly sensitive to the moisture and tend to hydrolyze to form dense precipitates prior to the cooperative assembly with the surfactants. Thus, traditional synthetic strategies for the mesoporous SiO<sub>2</sub>-based materials may not be applicable to the preparation of mesoporous metal oxides.);

(3) Structural collapses of the resultant mesoporous framework during the formation of crystallized phase and grain growth upon calcinations [52].

Dye-sensitized solar cells have become one of the major topics for next generation energy devices since highly efficient performances together with low cost were reported by Grätzel's group in 1991. The energy conversion efficiency of DSSC has been reported to reach 10–12%. These values have been obtained by using a liquid electrolyte as I<sup>-</sup>/I<sub>3</sub><sup>-</sup> – conducting element of the cells. However, several critical problems related to the presence of liquid media bring limitations to practical applications; Furthermore, solid-state or quasi solid-state DSSCs are advantageous over liquid based counterparts in terms of lightness, flexibility and long-term stability. Thus, there has been a great deal of research in the development of solid-state DSSC with higher efficiencies and long-term stability. However, the energy conversion



efficiencies of solid-state DSSCs are still lower than those of liquid-state DSSC. The basic reason is the lower ionic mobility of the redox species in the polymeric medium and poor interfacial contact between electrolytes and electrodes, which directly affects the cell performances. A recent alternative embodiment of the DSC concept is the sensitized heterojunction usually with an inorganic wide band gap nanocrystalline semiconductor of n-type polarity as electron acceptor, the charge neutrality on the dye being restored by a hole delivered by the complementary semiconductor, inorganic [54,55] or organic [56] and of p-type polarity. The prior photo-electrochemical variant, being further advanced in development, has an AM 1.5 solar conversion efficiency of over 10%, while that of the solid-state device is, as yet, significantly lower. Since the sensitizing dye itself does not provide a conducting functionality, but is distributed at an interface in the form of immobilized molecular species, it is evident that for charge transfer each molecule must be in intimate contact with both conducting phases. It is evident that this applies to the porous wide bandgap semiconductor substrate into which the photo-excited chemisorbed molecules inject electrons. It is also evident that in the photo-electrochemical format of the sensitized cell the liquid electrolyte penetrates into the porosity, thereby permitting the intimate contact with the charged dye molecule necessary for charge neutralization after the electron loss by exchange with the redox system in solution. It is not immediately evident that an interpenetrating network of two conducting solids can so easily be established that an immobilized molecule at their interface can exchange charge carriers with both. However, results are promising. The charge transport materials are deposited by spin coating from the liquid phase in order to achieve the necessary intimate contact, thereby introducing a solution of the conducting compound into the previously sensitized nanostructure. The charge transfer material currently used is a spirobifluorene.

### *2.82 The significance of the nanocrystalline film morphology*

A photovoltaic conversion system based on light harvesting by a molecular absorber attached to a wide band gap semiconductor surface faces two dilemmas. A monolayer of dye on a flat surface absorbs at most a few percent of light because it occupies an area that is much larger than its optical cross section. In quantitative terms the absorbance  $A$  of the dye covered film is given by:

$$A = \Gamma\sigma \quad (1)$$

where  $\Gamma$  (mol/cm<sup>2</sup>) is the surface coverage of the sensitizer and  $\sigma$  (cm<sup>2</sup>/mol) is the molar cross section for absorption of monochromatic light. The latter is the decadic molar extinction coefficient multiplied by 1000. Using a typical surface coverage of  $1 \times 10^{-10}$  mol/cm<sup>2</sup> and  $\sigma = 10^7$  cm<sup>2</sup>/mol one obtains  $A = 0.001$

Sensitizer films adsorbed on a flat surface absorb can only harvest a negligibly small fraction of the incoming light. The first embodiment of the dye-sensitized solar cell employed a TiO<sub>2</sub> film prepared by a sol-gel method, which had a surface roughness factor of about 150. Light scattering within the porous film structure further enhanced the light harvesting. Thus, the dye derivatized fractal TiO<sub>2</sub> films captured practically all the incoming photons with wavelength close to 470 nm, where the RuL3 sensitizer has its absorption maximum. Secondly compact oxide semiconductor films need to be n-doped to conduct electrons. However, the presence of conduction band electrons is undesirable as they can quench the excited sensitizer by energy transfer. This will inevitably reduce the photovoltaic conversion efficiency. Present embodiments of the DSC employ dye-derivatized oxide nanocrystals as light harvesting units in [57]. This provides a strikingly simple and powerful method to overcome these problems, which till recently have rendered solar energy conversion devices based on the sensitization of wide band gap oxides notoriously inefficient. The films are made of a network of undoped

(insulating) wide band gap oxide nanocrystallites producing a junction of huge contact area. For a 10 micro metre thick oxide film the surface is enlarged over 1000 times allowing for efficient harvesting of sunlight by the adsorbed monolayer of sensitizer. Thus, the fractal  $\text{TiO}_2$  film prepared by sol-gel chemical methods has been replaced with a nanostructure deposited from colloidal suspension. This evidently provides a much more reproducible and controlled porous high surface area texture. Further, since it is compatible with screen-printing technology, it anticipates future production requirements. While commercially available titania powders produced by a pyrolysis route from a chloride precursor have been successfully employed, the present optimized material is the result of a hydrothermal technique, described by Brooks and co-workers [58]. A specific advantage of the procedure is the ease of control of the particle size, and hence of the nanostructure and porosity of the resultant semiconductor substrate. The synthesis involves the hydrolysis of the titanium alkoxide precursor producing an amorphous precipitate followed by precipitation in acid or alkaline water to produce a sol which is subjected to hydrothermal Ostwald ripening in an autoclave. The resulting  $\text{TiO}_2$  particles consist of anatase or a mixture of anatase and rutile, depending on reaction conditions. The temperature of the hydrothermal treatment has a decisive influence on the particle size. The standard sol, treated for about 12 h at 230 °C in the autoclave has an average particle diameter of 20 nm as shown in Fig. 4. The prevailing structures of the anatase nanoparticles are square-bipyramidal, pseudocubic and stab like. According to HRTEM measurements the (1 0 1) face is mostly exposed followed by (1 0 0) and (0 0 1) surface orientations [59]. The formation of the (1 0 1) face is favoured by its low surface energy. The nanocrystalline  $\text{TiO}_2$  film in Fig. 4 was deposited by screen printing on a glass sheet covered by a transparent conducting oxide (TCO) that serves as current collector. The film thickness is typically 5–20  $\mu\text{m}$  and the  $\text{TiO}_2$  mass about 1–4  $\text{mg}/\text{cm}^2$ . Analysis of the layer morphology shows the porosity to be about 50–65%. In contrast to a compact oxide

layer there is no need to dope the oxide film since the injection of one single electron from the surface adsorbed sensitizer into a  $\text{TiO}_2$  nanoparticle is enough to turn the latter from an insulating to a conductive state. In addition, there is no space charge limitation on the photocurrent as the charge of the injected electrons can be effectively screened by the electrolyte surrounding the oxide nanocrystal. A striking and unexpected behaviour of the mesoporous  $\text{TiO}_2$  films is that the high surface roughness does not promote charge carrier loss by recombination. The reason for this behaviour is that the electron and the positive charge find themselves within picoseconds after light excitation of the dye on opposite sides of the liquid–solid interface [60]. The carrier loss mechanisms are comparatively slow, and although conventionally referred to as recombination, by analogy with the solid-state process, the loss of a photo-excited electron from the semiconductor should be regarded as a recapture, by an oxidized dye species or a the oxidized form of the redox couple in the electrolyte. Either occurs on a micro- to millisecond time scale. Finally if a hole conductor is employed instead of the electrolyte the electrons and holes are injected in the nanocrystalline oxide film and hole conductor, respectively. Hence, their recombination can be controlled by the interface.

### ***2.83 The choice of the sensitizer***

The ideal sensitizer for a single junction photovoltaic cell converting standard global AM 1.5 sunlight to electricity should absorb all light below a threshold wavelength of about 920 nm. In addition, it must also carry attachment groups such as carboxylate or phosphonate to firmly graft it to the semiconductor oxide surface. Upon excitation it should inject electrons into the solid with a quantum yield of unity. The energy level of the excited state should be well matched to the lower bound of the conduction band of the oxide to minimize energetic losses during the electron transfer reaction. Its redox potential should be sufficiently

positive so that it can be regenerated via electron donation from the redox electrolyte or the hole conductor. Finally, it should be stable enough to sustain about 10<sup>8</sup> turnovers corresponding to 20 years of lifetime.

#### ***2.84 Spectrum utilization***

Another strategy to obtain a broad optical absorption extending throughout the visible and near IR region is to use a combination of two dyes which complement each other in their spectral features. Such dye cocktails have already been applied to mesoporous TiO<sub>2</sub> films in the form of mixtures of porphyrines and phthalocyanines. The result was encouraging in as much as the optical effects of the two sensitizers were found to be additive. In particular, there was no negative interference between the co-adsorbed chromophores opening up the way for testing a multitude of other dye combinations [61]. Semiconductor quantum dots are another attractive option for panchromatic sensitizers. These are II–VI and III–V type semiconductor particles whose size is small enough to produce quantum confinement effects. The absorption spectrum of such quantum dots can be adjusted by changing the particle size. Thus, the band gap of materials such as InAs and PbS can be adapted to match the value of 1.35 eV, which is ideal for a single-junction solar quantum converter. During the last decade a wealth of information has been gathered on the physical properties of these materials and the research is being pursued very actively. One problem with this approach is the photo-corrosion of the quantum dots, which will almost certainly happen if the junction contact is a liquid redox electrolyte. However, they are expected to display higher stability in the solid-state heterojunction device [62]. The advantage of these sensitizers over conventional dyes is their very high extinction coefficient allowing for use of thinner films of the mesoporous oxide. This should reduce the dark current increasing  $V_{oc}$  and the overall efficiency of the cell.

## 2.85 Charge percolation

When the dye-sensitized nanocrystalline solar cell was first presented perhaps the most puzzling phenomenon was the highly efficient charge transport through the nanocrystalline TiO<sub>2</sub> layer. The mesoporous electrodes are very much different compared to their compact analogs because

- (i) The inherent conductivity of the film is very low,
- (ii) The small size of the nanocrystalline particles does not support a built-in electrical field
- (iii) The electrolyte

The electrolyte penetrates the porous film all the way to the back-contact making the semiconductor/electrolyte interface essentially three-dimensional. Charge transport in mesoporous systems under keen debate today and several interpretations based on the Montrol–Scher model for random displacement of charge carriers in disordered solids [63] have been advanced. However, the “effective” electron diffusion coefficient is expected to depend on a number of factors such as trap filling and space charge compensation by ionic motion in the electrolyte. Therefore, the theoretical and experimental effort will continue as there is a need for further in depth analysis of this intriguing charge transport process. The factors controlling the rate of charge carrier percolation across the nanocrystalline film are presently under intense scrutiny. Intensity modulated impedance spectroscopy has proved to be an elegant and powerful tool [64,65] to address these and other important questions related to the characteristic time constants for charge carrier transport and reaction dynamics in dye-sensitized nanocrystalline solar cells. Very interestingly, recent pulsed laser-induced current transient measurements carried out in Prof. Yanagida’s laboratory have revealed that dye adsorption onto nanoporous TiO<sub>2</sub> electrode can increase the electron diffusion coefficient compared with a bare surface [66].

### ***2.86 Advanced mesoporous materials nanotubes and nanobrushes***

On the material science side, research is currently being directed towards synthesizing structures with a higher degree of order than the random assembly of nanoparticles. A desirable morphology of the films would have the mesoporous channels or nanorods aligned in parallel to each other and vertically with respect to the TCO glass current collector. This would facilitate charge diffusion in the pores and the mesoporous film, give easier access to the film surface, avoid grain boundaries and allow the junction to be formed under better control. One approach to fabricate such oxide structures is based on surfactant templates assisted preparation of TiO<sub>2</sub> nanotubes as described in paper by Adachi et al. [67]. Very recently a simple approach to prepare oriented nanobrushes of TiO<sub>2</sub> on titanium supports has been published [68]. The work of Alivisatos and coworkers [69] on hybrid solar cells consisting of blends of CdSe nanoparticles with polythiophene has confirmed the superior photovoltaic performance of nanorod films with regards to random networks of spherical particles

### ***2.87 Mastering the interface***

The high contact area of the junction nanocrystalline solar cells renders it mandatory to grasp and control of interfacial effects for future improvement of cell performance. The nature of the exposed surface planes of the oxide and the mode of interaction with the dye is the first important information to gather. For the adsorption of the N3 dye on TiO<sub>2</sub> this is now well understood. The prevalent orientation of the anatase surface planes is (1 0 1) and the sensitizer is adsorbed through two of the four carboxylate groups, at least one of them being anchored via a bidentate configuration bridging two adjacent titanium sites. Molecular dynamic calculations employing a classical force field have been carried out to predict the equilibrium geometry of the adsorbed sensitizer state [70]. More sophisticated first principle density

functional calculations have also been launched recently to model the surface interactions of  $\text{TiO}_2$  with simple adsorbates as well as the surface reconstruction effects resulting from the adsorption. The latter approach is particularly promising and will provide an important tool for future theoretical investigations. Synthetic efforts focus on the molecular engineering of sensitizers that enhance the charge separation at the oxide solution interface. The structural features of the dye should match the requirements for current rectification: in analogy to the photo-field effect in transistors, the gate for unidirectional electron flow from the electrolyte through the junction and into the oxide is opened by the photo-excitation of the sensitizer. The reverse charge flow, i.e. recapture of the electron by the electrolyte could be impaired by judicious design of the sensitizer. The latter should form a tightly packed insulating monolayer blocking the dark current. For each order of magnitude decrease in the dark current the gain in  $V_{oc}$  would be 59mV at room temperature. The 15% limit with the currently employed redox electrolytes. Important progress to control the self-assembly of the N3 dye at the  $\text{TiO}_2$  interface was achieved recently in our laboratory. The strategy employed was to add guanidinium thiocyanate to the electrolyte. The guanidinium cations are adsorbed along with the N3 anions at the interface, screening the lateral Columbic repulsion of the sensitizer and facilitating in this fashion the self-assembly of a compact dye monolayer. This results indeed in a remarkable improvement of the cell voltage due to a reduction in dark current. Using this approach, a new record conversion efficiency of 11% was achieved recently. Work in this direction is indispensable to raise the efficiency of the DSC significantly over with these cells.

**2.88 Nanocrystalline and mesoporous materials**-Transporting electrons through the conduction band of titania would not be efficient, because the electrons have to pass through



numerous grain boundaries in order to reach the transparent conducting oxide (TCO). The structural disorder at the contact between two crystalline nanoparticles also leads to enhanced scattering of free electrons, thus reducing electron mobility. In addition, the transport of electrolytes, especially ionic liquids, is inefficient because of the irregularity of the pore network. Consequently, tailoring of a porous titania structure at nanoscale levels in order to expedite the transport of both electrons and electrolytes is crucial to increasing the overall performance of DSSCs. In this regard, a long-range ordered mesoporous titania film is a promising candidate as the nanoporous electrode of DSSC, because of its high specific surface area, uniform pore morphology with excellent connectivity of mesopores, beneficial to the electrolyte diffusion and an interconnected titania skeleton with regularly packed nanocrystalline particles, desirable for an efficient charge carrier transport. Evaporation-induced self-assembly (EISA) is an effective technique for preparing highly ordered mesoporous titania. This technique was initially proposed for the preparation of mesoporous silica thin films. It was then devised by Stucky *et al* for synthesis of mesoporous transition metal oxides with organized mesostructure. By using this technique, supramolecular templates, typically amphiphilic surfactant molecules or copolymers composed of hydrophobic and hydrophilic building blocks, self-assemble into a liquid crystalline mesophase surrounded by an inorganic oxide network, which is formed via the sol-gel route. However, there has been limited success in the application of supramolecular templated mesoporous titania in DSSCs, as a result of the combination of several unsolved technical issues.

Firstly, the mesoporous titania films prepared by EISA were of submicrometer thickness, only (100–300 nm), which provides insufficient surface area rendering poor light harvesting by the monolayer of adsorbed dyes on the titania surface. To realize thicker films, multilayered titania films were prepared using the doctor-blading method, but the films lost their structural

ordering and exhibited a wormlike mesostructure. Titania films of 1  $\mu\text{m}$  in thickness with ordered cubical mesoporous structure were fabricated using a layer-by-layer deposition process by dip coating three times. Their DSSC performance using N719 as the sensitizer showed a maximum efficiency of 2.95%, higher than that of the conventional oxide films of a similar thickness made of randomly clustered anatase nanocrystals. The cell performance of thicker films were however not reported. During the layer-by-layer deposition, the surface area would not increase after depositing more than 3–5 layers, because the new surface area added by the further deposition of a top layer was compensated by the surface area lost due to the sintering of the bottom layers. Consequently, pore accessibility becomes the second problem, limiting the dye adsorption and the electrolyte percolation due to pore blocking. Thirdly, the templated titania often exhibits a semicrystalline network with the coexistence of anatase nanocrystals and a significant amount of amorphous titania. It has been reported that the low crystallinity of the surfactant-templated titania matrix always leads to low solar conversion efficiencies [71].

Kinetics of electron injection into the semiconductor photoelectrode after being excited from the photosensitizer has been investigated by many researchers using time-resolved laser spectroscopy (Hara & Arakawa, 2003). It has been found that both the configuration of the photosensitizer material and the energy separation between the conduction band level of the wideband gap semiconductor and the LUMO level of the photosensitizer are greatly affecting the electron transfer rate to the wideband gap semiconductor. Investigations have been done to evaluate excitation of the dye from the HOMO to the LUMO level, relaxation of the excited state (60 ns), electron injection from the dye LUMO level to the  $\text{TiO}_2$  conduction band (50 fs - 1.7 ps), recombination of the injected electron with the hole in the dye HOMO level (ns - ms), recombination of the electron in the  $\text{TiO}_2$  conduction band with a hole ( $\text{I}_3^-$ ) in the electrolyte (10 ms), and the regeneration of the oxidized dye by  $\text{I}^-$  (10 ns). (Hagfeldt &

Gratzel, 2000). It has been confirmed that electron injection from the excited dye such as the N3 dye or RuL2 (NCS)<sub>2</sub> complex into the TiO<sub>2</sub> conduction band (CB) is a very fast process in femtosecond scale. The reduction of the oxidized dye by the redox electrolyte's I<sup>-</sup> ions occur in about 10<sup>-8</sup> seconds. Recombination of photoinjected CB electrons with oxidized dye molecules or with the oxidized form of the electrolyte redox couple (I<sub>3</sub><sup>-</sup> ions) occurs in microseconds (Hara & Arakawa, 2003). To achieve good quantum yield, the rate constant for charge injection should be in the picosecond range. In conclusion, Fast recovery of the sensitizer is important for attaining long term stability. Also, long-lasting charge separation is a very important key factor to the performance of solar cells. Thus, new designs for larger conjugated dye-sensitizer molecules have been reported by investigators ,for example, Haque et al., (Haque et al., 2004) studied hybrid supermolecules that are efficiently retard the recombination of the charge-separated state and therefore assure enhanced energy conversion efficiency by extending the lifetime of light-induced charge-separated states. Hybrid supermolecule is the structure of the redox triad that gave the most efficient charge separation in the report by Haque and colleagues. The triad is made of a ruthenium complex anchored to nanocrystalline TiO<sub>2</sub> (the electron acceptor) and covalently linked to polymeric chains of triphenyl-amine groups (the electron donor). Arrows represent the direction of the electron transfer process. The first step of the electron transfer is the light-induced excitation of the chromophore; following this an electron is readily injected from the sensitizer excited state into the conduction band of the TiO<sub>2</sub> semiconductor (process 2). The direct recombination of primarily separated charges would degrade the absorbed energy into heat.

In this supermolecule this is avoided through the fast reduction of the ruthenium by the linked triphenyl-amine electron donor groups. The secondary recombination process between the injected electron and the oxidized amine radical is made increasingly slow because the

positive charge can hop from one triphenylamine function to the adjacent one along the chain and the hole moves away from the TiO<sub>2</sub> surface. The overall photo-initiated process thus results in unidirectional electron flow from the end of the polymeric chains to the oxide and a very long-lived charge-separated state” (Moser, 2005). In TiO<sub>2</sub> nanoparticle DSSCs, the electrons diffuse to the anode by hopping 10<sup>3</sup>-10<sup>6</sup> times between particles (Baxter et al., 2006). With each hop there is a considerable probability of recombination of the photoexcited electron with the electrolyte since both the diffusion and recombination rates are on the order of milliseconds. Hence, this allows recombination to limit the cell efficiency. On the other hand, nanowire or tube structured photoelectrode (e.g., ZnO<sub>2</sub>) provide a direct path (express highway) to the anode, leading to increased diffusion rate without increasing the recombination rate and thus increases cell efficiency. The sensitizer molecule adsorbed to a nanostructured TiO<sub>2</sub> surface promise to improve the photovoltaic conversion efficiency of dye sensitized solar cell (From Moser, 2005). Dark current in DSSC is mainly due to the loss of the injected electron from nanostructured wide bandgap semiconductor (say TiO<sub>2</sub>) to I<sub>3</sub> (the hole carrier in solution electrolyte). Thus, it is a back reaction that must be eliminated or minimized. Reduction of dark current enhances the open circuit voltage of the cell, this can be deduced from the following general equation of solar cell relating the open circuit voltage V<sub>OC</sub> to both the injection current I<sub>inj</sub> and dark current I<sub>dark</sub>.

### **2.89 Applications and commercialization of DSSC**

Because of the physical nature of the dye sensitized solar cells, inexpensive, environment friendly materials, processing, and realization of various colours (kind of the used sensitizing dye); power window and shingles are prospective applications in building integrated photovoltaics BIPV. The Australian company Sustainable Technologies International has produced electric-power-producing glass tiles on a large scale for field testing and the first

building has been equipped with a wall . The availability of lightweight flexible dye sensitized cells or modules are attractive for 194 Solar Cells – Dye-Sensitized Devices applications in room or outdoor light powered calculators, gadgets, and mobiles. Dye sensitized solar cell can be designed as indoor colorful decorative elements .Flexible dye sensitized solar modules opens opportunities for integrating them with many portable devices, baggage, gears, or outfits . In power generation, dye sensitized modules with efficiency of 10% are attractive choice to replace the common crystalline Si-based modules. [72]

Commercialization of dye sensitized solar cells and modules is taking place in almost all Continents. In Asia, specifically in Japan: IMRA-Aisin Dye Sensitized Solar Cells Seiki/Toyota, Sharp, Toshiba, Dai Nippon, Peccell Technologies are frontrunners. In Australia: Dyesol, In USA Konarka., G24i in UK, and Solaronix in Switzerland. G24i has announced a DSC module production of 25MW capacity in 2007 in Cardiff, Wales (UK), with extension plans up to 200MW by the end of 2008 (<http://www.g24i.com>). The success of many labs and companies such as ASIAN and Toyota Central R & D Labs., INC, to demonstrate various sizes and colours in a series-connected dye solar cell module in many international exhibitions and conferences reflects the potential role of dye sensitized solar cells systems in the PV technology. In fact, Toyota has installed in their dream house walls a similar kind of DSSCs panels, an example of DSSC module for outdoor application (From <http://kuroppe.tagen.tohoku.ac.jp/~dsc/cell.html>). Glass substrate is robust and sustains high temperatures, but it is fragile, nonflexible, and pricey when designed for windows or roofs. Flexible DSSCs have been intensively investigated. Miyasaka et. al. (Miyasaka & Kijitori, 2004) used the ITO (indium tin oxide) coated on PET (polyethylene terephthalate) as the substrate for DSSCs. Generally, the conducting glass is usually coated with nanocrystalline  $\text{TiO}_2$  and then sintered at 450 - 500 degree Celcius to improve the electronic contact not only between the particles and support but also among the particles. Plastics films

have a low ability to withstand heat. The efficiency of plastic-based dye sensitized solar cells is lower than that of using glass substrate ( $\eta = 4.1\%$ ,  $J_{sc} = 9.0 \text{ mA/cm}^2$ ,  $V_{oc} = 0.74 \text{ V}$ ,  $FF = 0.61$ ) because of poor necking of  $\text{TiO}_2$  particles. Kang et al., (Kang et al. 2006), used the stainless steel as the substrate for photoelectrode of DSSCs. The cell illuminated through the counter electrode due to the non-penetration of light through metal substrate. In their system, the  $\text{SiO}_x$  layer was coated on stainless steel (sheet resistance  $\sim 1 \text{ ohm per metre square}$ ) and separated ITO from stainless steel, for preventing photocurrent leakage from stainless steel to the electrolyte. The constructed cells resulted in  $J_{sc} = 12 \text{ mA/cm}^2$ ,  $V_{oc} = 0.61 \text{ V}$ ,  $FF = 0.66$ , and  $\eta = 4.2 \%$ . Recently, Chang et al. fabricated flexible substrate cell that produced conversion efficiency close to 2.91%. The photoelectrode substrates are flexible stainless steel sheet with thickness 0.07mm and titanium (Ti) sheet with thickness 0.25mm (Chang et al., 2010). Also, the reported approach by Yen et al. in developing a low temperature process for the flexible dye-sensitized solar cells using commercially available  $\text{TiO}_2$  nanoparticles (such as P25) is interesting since it yielded a conversion efficiency of 3.10% for an incident solar energy of  $100 \text{ mW/cm}^2$  (Yen et al. 2010). Because Titanium has extremely high corrosion resistance, compared with stainless steel, titanium is still the privileged substrate material. A prototype of a flexible dye sensitized solar cell using stainless steel substrate has been designed (From Kang et al., 2006). Availability of non-volatile electrolyte is another issue toward commercialization of single or multi-junction modules. Polymer (solid) electrolyte, hole conductor, and solidified ionic liquids are solvent free choices with high electronic conductivity and chemical stability (Wang et al., 2005.) The key to high power heterojunction DSSC is to increase the effective diffusion length of electron within the nanostructured electrode by increasing the mobility of hole conductor or the extinction coefficient of the sensitizer to ensure more efficient light harvesting action. Since heat and UV light degrade cells performance, development of heat sink and optimized low cost UV coating is a must for

outdoor applications. The successes in development of flexible substrate, solid electrolyte, and spectrally broad absorption range inexpensive nontoxic dyes will potentially open the possibility of role-to-role mass production of dye sensitized solar cells and modules.

Molecular engineering of efficient and stable organic sensitizers is an open invitation for many research groups, the successes in this area is expected to advance production and commercialization of DSSC (Kim et al., 2006). . Nanocrystalline dye sensitized solar cell DSSC is classified as a low cost, environmental friendly, and capable of being highly efficient cell mainly due to materials, charge carriers generation and transport within the cell structure.

The nanostructured dyesensitized solar cell (DSSC) is going to provide economically credible alternative to present day p–n junction photovoltaics. In fact, dye sensitized solar cell are green solar cell mimicking the green leave. In dye sensitized solar cell electricity is generated as a result of electron transfer due to photoexcitation of dye molecules adsorbed to nanostructured wide bandage material photoelectrode. The oxidized dye molecules regenerated by gaining electrons from electrolyte which is reduced by the electrons reaching the counter-electrode of the cell. In dye sensitized solar cells light absorption is separated from carrier transport. From educational point of view, since nanostructured dye sensitized solar cell DSSC is mimicking photosynthesis in plants, it provides an interdisciplinary context for students learning the basic principles of biological extraction, chemistry, physics, environmental science and electron transfer. The requirements of practical sensitizers are: broad band and high level absorption of visible and near infrared region of the electromagnetic spectrum, exhibit thermal and photochemical stability, chelating to the semiconductor oxide surface and inject electrons into the conduction band with a quantum yield of unity, and owning suitable ground- and excited state redox properties. Investigations of solvent free electrolyte such as polymer based, and ionic liquid are promising. In order to commercialize dye sensitized solar cell in low power applications, flexible DSSCs have been

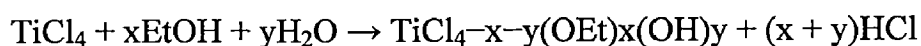
intensively investigated. The solar to electric power conversion efficiency of the DSC in full AM 1.5 sun light validated by accredited PV calibration laboratories has reached over 11 % and modules with efficiency close to 10% has been exhibited in 2010. Nanowires and quantum dots QDSSCs may be a promising solar cell design. The search for green sources or generators of energy is considered one of the priorities in today's societies and occupies many policy makers' agendas. We at the University of Bahrain are the first to start the investigation of Dye sensitized solar cells DSSCs in the Arabian Gulf. Dye sensitized solar cells using natural organic dyes were prepared using low cost materials and natural dyes. Sensitization of wide gap oxides semiconductor materials was accomplished with the growth of nanocrystalline  $\text{TiO}_2$ . The natural dyes extracted from Henna (*Lawsonia inermis* L.), pomegranate, cherries, and raspberries (*Rubus* spp.). It has been found that the nanocrystalline material based solar cell system exhibits an excellent optical absorption parameters for visible and near infrared portion of the electromagnetic spectrum. The performance of natural dye extract sensitized nanocrystalline solar cells can be appreciably enhanced by optimizing preparation technique, using different types of electrolyte, reported additives, and sealing. In short, compared to Si based solar cells dye sensitized solar cells are of low cost and ease of production, their performance increases with temperature, possessing bifacial configuration - advantage for diffuse light, have transparency for power windows, colour can be varied by selection of the dye, invisible PV-cells based on near-IR sensitizers are feasible, and they are outperforms amorphous Si. Moreover, DSSC shows higher conversion efficiency than polycrystalline Si in diffuse light or cloudy conditions. It is believed that nanocrystalline photovoltaic devices are becoming viable contender for large scale future solar energy converters. [72]

**2.9 Selection of appropriate starting materials-** Selection of appropriate starting materials, especially the Ti source and block copolymer, is vital in the successful preparation of highly



organized mesoporous structure of TiO<sub>2</sub> films. The suitable Ti source is quite limited. Only anhydrous TiCl<sub>4</sub> or concentrated acid stabilized titanium alkoxides are acceptable for the synthesis of highly organized mesoporous TiO<sub>2</sub> films. Available titanium alkoxides include titanium ethoxide (Ti(OEt)<sub>4</sub>), titanium isopropoxide (Ti(O-iPr)<sub>4</sub>), and titanium butoxide (Ti(OBu)<sub>4</sub>), listed in an order of increasing reactivity in hydrolysis. Compared with other Ti sources such as Ti(SO<sub>4</sub>)<sub>2</sub> and TiF<sub>4</sub>, they have predominant performances in controlling the homogeneity of initial solution and final size of TiO<sub>2</sub> crystallites on the nanoscale. For the suitable block copolymers, commercially available amphiphilic poly(ethylene oxide)-block-poly(propylene oxide)-block-poly(ethylene oxide) (PEO-PPO-PEO) tri-block copolymers, typically Pluronic P123 (PEO<sub>20</sub>PPO<sub>70</sub>PEO<sub>20</sub>, and F127 (PEO<sub>106</sub>PPO<sub>70</sub>PEO<sub>106</sub>, consisting of a central hydrophobic PPO chain and two hydrophilic PEO tails, have been widely used as the structure-directing agents for the construction of highly organized mesoporous structure for TiO<sub>2</sub>, where P and F stand for the physical form of paste and flake, respectively.

**2.10 Initial sol solution preparation-** Homogenous initial sol solution can be prepared by dissolving the anhydrous TiCl<sub>4</sub> or stabilized titanium alkoxides into the alcohol-rich solution containing suitable amount of water and pre dissolved block copolymer. The sol-gel reaction of TiCl<sub>4</sub> in the initial sol solution can be described as follows:



The in-situ generated HCl during the hydrolysis induces a strongly acidic condition, which can sufficiently suppress further hydrolysis and poly condensation reaction of TiCl<sub>4-x-y</sub>(OEt)<sub>x</sub>(OH)<sub>y</sub>. Titanium alkoxides are another kind of popular Ti sources, which can be handled more conveniently than TiCl<sub>4</sub>. Different from TiCl<sub>4</sub>, that enables to create strongly acidic condition to achieve self-stabilization, titanium alkoxides should be pre-stabilized by acids before mixing with block copolymer-containing solution. Concentrated hydrogen chloride (HCl, 35–37 wt%) with a HCl/Ti molar ration of 1.6–2.0 is most

commonly employed to control the hydrolytic reactivity of titanium alkoxides. Other acids, sulphuric acid, nitric acid, phosphoric acid, and acetic acid have also been used in stabilizing Ti precursor in order to eliminate the accommodation of  $\text{Cl}^-$  in resulting films. HCl not only can provide a strongly acidic medium, but also easily forms complexes with titanium alkoxides.

**2.11 Film deposition-** In depositing the initial sol solution on the substrate, coating method is critical for the long-range ordering of the fabricated mesoporous  $\text{TiO}_2$  films. Henrist et al. prepared mesoporous thin films with various thickness by adjusting the withdrawal speed during dip-coating, and found that a slow-speed dip-coating allows to obtain mesoporous  $\text{TiO}_2$  films with thinner thickness, smoother surface, and higher regularity and porosity. Similar conclusions were also drawn in spin-coating process. The long-range ordering of mesoporous  $\text{TiO}_2$  films can be greatly affected by the environmental relative humidity (RH) during deposition and aging process. Sanchez's group found that the initial films dip-coated at high RH are transparent, but the aged films present a non-homogeneous thickness due to the difficulty in controlling the solvent evaporation from area to area in the films. On the other hand, films deposited in  $\text{RH} < 45\%$  are of excellent optical quality, but present a worm-like mesostructure. A combination process was thus developed to synthesize highly organized cubic mesoporous  $\text{TiO}_2$  with high transparency. That is, a low RH of 30% was applied for film deposition and immediately RH was changed to 50% during the subsequent humidity aging process. In contrast, Kwon's and Schouten's groups investigated humidity control during spin-coating process, and found that a high humidity ( $\text{RH} = 70\text{--}80\%$ ) is required to improve the regularity of the cubic mesoporous structures. The disagreement in conclusion is closely related to coating method accompanied by distinct characteristics of solvent evaporation. In dip coating process, without the external driving force inducing the evaporation, a low-RH condition is beneficial to the as-deposited film reaching its dry line,

whereas a high-RH condition will be favourable for the spin coated film, since it facilitate a relatively much more energetic volatilization regardless the atmospheres .The deposited hybrid coating can directly reach its dry line after spin-coating and launches self-assembly process. In this case, a dried condition may retard the mobility of resident species and thus the self-assembly between nano building blocks (NBB) and block copolymers, lowering the ordering of the fixed mesostructure.

**2.12 Humidity aging-** The as-deposited films remain liquid crystalline phases with a fragile mesostructure, since the NBB are almost uncondensed due to the high acidity of initial sol solution. To consolidate the mesostructure, hybrid films should be exposed in a humid atmosphere under a constant relative humidity (RH), allowing residual HCl and other volatile components completely evaporated from films. With the absorption of the moisture, NBB are hydrolyzed and polycondensed, and Cl<sup>-</sup> and alkoxides ligands associative to Ti are substituted by -OH group gradually. The increase in the interfacial hydrophilicity promotes the penetration of hydrophilic block into the inorganic frameworks, enhancing the crosslink between block copolymer and inorganic species and in turn improving the thermal stability of mesostructured TiO<sub>2</sub> films. Another important role of humidity aging is to reserve the flexibility and mobility of block copolymers for self-assembly and mesostructural organization .Experimentally, aging of the coated film can be carried out in an electronic humidity chamber, dry keeper, or close chamber with saturated salt solution. A proper aging condition should result in highly transparent films without any observable white precipitation on the film surface since the stabilized Ti species show excellent resistance to moisture. Clearly RH value, aging period and aging temperature are three key parameters during humidity aging. Over high RH and/or aging period and/or aging temperature may cause extreme hydrolysis and poly-condensation of inorganic species in the hybrid framework. Upon calcination, the long-range ordering of mesoporous structure will be deteriorated due to

the generation of large TiO<sub>2</sub> nanocrystallites. In the opposite situation, decrease in flexibility of surfactant and insufficient hydrophilic NBB hinder their cooperative assembly in the liquid crystal phase. Several research groups have verified that the optimal RH value is at the range of 50–80%, aging period is 1–3 days], and aging temperature is 5–25 °C.

**2.13 Thermal treatment** -Long-range ordered mesoporous structures can be generated by calcining the pre-organized mesoporous hybrid films in static air at an elevated temperature ( $\geq 300$  °C) at a slow ramping rate (generally 1 °C/min). Additionally, Schouten's group found that a low residual pressure (ca. 10 mbar) would be beneficial to preserving the mesoporous structure. The intimate interaction between the block copolymer and NBB increases the decomposition temperature for block copolymer templates to 200–280 °C. Before removal of organic templates, films must be baked at the temperatures of 60–200 °C for certain periods to ensure the full polycondensation of NBB. Considerable mesostructural shrinkages occur upon calcinations as a result of the generation of stress due to the surfactant removal and the formation of more dense structure with crystallization of inorganic framework. Sanchez's group applied in-situ thermal ellipsometric analysis to investigate the pyrolysis, crystallization, and sintering of mesoporous TiO<sub>2</sub> thin films. They found that slow heating rate resulted in a lower crystallization temperature and less shrinkage of mesostructure with lower refraction index. Thus, a gentle ramp rate of 0.5–2 °C/min was accepted as a suitable temperature program. After complete removal of templates at 300 °C, an elevated ramp rate (e.g. 5–10 °C/min) and short calcination time at target temperature (300–700 °C) were applied to prevent the extensive crystal growth. By such optimization, the resultant mesoporous TiO<sub>2</sub> films could keep their highly organized mesoporous structure even at 700°C.

**2.14 Mesophase control**-Apart from the composition control in the initial sol solution, deposition condition, RH value during aging, and thermal treatment procedure are able to control the mesophase in the mesoporous TiO<sub>2</sub> films. Coating method enables to vary

evaporation speed during the film deposition. Low evaporation speed by dip-coating, slow-speed spin-coating induces a cubic mesophase since enough ethanol and H<sub>2</sub>O can remain in the as-coated films to decrease volume fraction of block polymer, whereas high-speed spin-coating leads to a hexagonal mesophase.

### **2.15 Photo- electrochemical and catalytic applications of mesoporous TiO<sub>2</sub>- based films-**

The large surface area, pore-wall structure, crystallinity, and controllable components favoured mesoporous TiO<sub>2</sub>-based films for many promising applications. Their applications are highlighted in the photo- and electro-chemical field, including photocatalysis, dye-sensitized solar cell, electro-chromic and photo- electrochromic devices, and .Other applications are chemical energy storage (e.g. Li ion batteries and supercapacitors, luminescent devices, drug delivery and advanced materials design.

**2.16 Photocatalysts-** By absorption of the light with greater photonic energy than the band gap, semiconductors will generate electron-hole pairs, which initiate simultaneously oxidative and reductive reactions with surface species before recombination. Thereby the so-called semiconductors-mediated heterogeneous photocatalysis has received considerable attention, since the production of hydrogen from the water with TiO<sub>2</sub> electrode. Due to its adequate band gap and position, high quantum efficiency based on low electron-hole recombination rate, non toxicity, low cost, long-term stability, and others, TiO<sub>2</sub> has been demonstrated one of the most preferable semiconductors exhibiting considerable efficiency at ambient temperature in photo-catalytic oxidization of organic contaminations to environmentally benign products, such as CO<sub>2</sub>, H<sub>2</sub>O, and mineral acid and in the inactivation of microorganisms, such as bacteria and viruses .Mesoporous TiO<sub>2</sub> films, possessing the open pore channels with high connectivity and large external surface area can be a suitable architecture for these applications.

**2.17 Photocatalytic performances of mesoporous TiO<sub>2</sub> films-** Despite their low crystallinity, mesoporous TiO<sub>2</sub> films have demonstrated remarkably high photocatalytic activities than the nonporous films in water splitting and in complete degradation of organic contaminations. Excellent water disinfection property of mesoporous TiO<sub>2</sub> films was also found in killing *Escherichia coli*, a representative bacterium widely existing in the aquatic environment. The superior performances of mesoporous TiO<sub>2</sub> films in various photocatalytic reactions are mainly attributed to their large accessible surface area and well-defined mesopores with uniform pore size and excellent connectivity, in which both effective charge carrier transfer and efficient mass flow of the reactants and products can be easily achieved. Calcination temperature for highly organized mesoporous TiO<sub>2</sub> films should be optimized, since it strongly influences the textural property and thereby the photocatalytic activity. With increase of calcination temperature, mesoporous TiO<sub>2</sub> frameworks gradually crystallize and shrink, leading to decrease in the surface area while increase in crystallinity, crystal size, and pore diameter. Thus, the calcination temperature has to be adjusted to balance these parameters in order to achieve a highest photocatalytic activity. The effect of mesophases on the photocatalytic activity of mesoporous TiO<sub>2</sub> films was also explored. Lee's group found that the 3-D cubic mesoporous TiO<sub>2</sub> film showed a relatively higher photocatalytic activity in photocatalytic decomposition of 2-propanol in gas phase as compared to 2-D hexagonal one. Adsorption is regarded as a rate-determining step in the gas-phase photocatalytic reaction. Therefore, 3-D cubic mesoporous TiO<sub>2</sub> films shows much advance in photocatalysis because it holds greater accessibility and one more dimension for mass transfer of pollutant molecules and products. Similar results were also obtained when the adsorption ability and photocatalytic activity of 2-D and 3-D hexagonal mesoporous TiO<sub>2</sub> films were compared. The accessible surface area of 3-D hexagonal mesoporous TiO<sub>2</sub> film estimated by the adsorption of methylene blue was found to be nearly twice as large as that of 2-D hexagonal one.

Photocatalytic TiO<sub>2</sub> coatings on various substrates present value-added self-cleaning and super-hydrophilic properties. To integrate anti-reflectivity, water-repellence, antifogging, and self-cleaning functions in the resulting coated glass, an oxide bilayer has been designed. The bilayer consisted of a transparent, water resistant, hybrid methyl-functionalized nanoporous SiO<sub>2</sub> thin layer covered with an ultrathin mesoporous TiO<sub>2</sub> nanocrystalline film which acted as a protecting barrier toward mechanical aggressions and assures high water wetting (anti-fogging) and photocatalysis (self-cleaning) at the surface. Practical application of mesoporous TiO<sub>2</sub> films in photocatalytic membrane filtration has been recently studied by Ayrál's group. Highly organized cubic mesoporous TiO<sub>2</sub> films deposited on the surface of ceramic symmetric membranes showed a comparable photocatalytic activity to that of Degussa P25. As a result, the resulting membrane possessed an anti-fouling property. Additionally, the permeate flux of the membrane was not significantly decreased since the upper 3D cubic mesoporous structure was favourable for water to pass through the mesoporous TiO<sub>2</sub> films without high resistance.. Rational design of mesoporous TiO<sub>2</sub>-based films as efficient photocatalysts to further maximize the photocatalytic activity of TiO<sub>2</sub> under UV or visible light irradiation, several design strategies have been applied to the photocatalytic TiO<sub>2</sub> system, including doping with metal ions (e.g. Fe<sup>3+</sup>, Cr<sup>3+</sup>) or anion (e.g. N, F, C, S, B), coupling with metals (e.g. Pt, Au, Ag) or semiconductors (e.g. WO<sub>3</sub>, SiO<sub>2</sub>, SnO<sub>2</sub>, CdS), and surface functionalizations. By stabilizing the highly reactive tungsten(V) ethoxide with complexing agent of cetylacetate, Lee and co-workers prepared long-range ordered cubic mesoporous WO<sub>3</sub>/TiO<sub>2</sub> thin films.

**2.18 Deposition of mesoporous TiO<sub>2</sub> thick films by doctor blade method** –Doctor- Blade of nanocrystalline TiO<sub>2</sub> paste is the typical film coating technique used to fabricate DSSC photo-anode with a controllable thickness. However, this method is unable to directly transfer the Ti-sol solution to conductive substrate since the diluted solution has a very low viscosity.

Mesoporous TiO<sub>2</sub>-based films loaded with Pt nanoparticles as a counter electrode of DSSC. To increase the active surface area of Pt counter electrode, Wu's group impregnated Pt nanoparticles into mesoporous Nb-doped TiO<sub>2</sub> film deposited on FTO. Owing to the high dispersion of Pt nanoparticles and the increased conductivity of the film by the loaded 1mol% Nb, the resulting Pt/Nb-doped TiO<sub>2</sub> film, showed promising electrocatalytic activity for the I<sub>3</sub><sup>-</sup>/I<sup>-</sup> redox reaction in acetonitrile by decreasing the charge transfer resistance and increasing exchange current density[55].

**2.19 Layer-by-layer deposition of mesoporous TiO<sub>2</sub> film-** Due to the low viscosity and dilute concentration for the initial Ti-sol solution, the thickness of mesoporous TiO<sub>2</sub> films synthesized via evaporation induced self assembly (EISA) process is in the range of 200–500nm per coating, which is more than one order lower than the typical thickness (generally 10 micro metre) of nanocrystalline TiO<sub>2</sub> films providing the optimum photovoltaic efficiency in DSSC. To increase the TiO<sub>2</sub> thickness and then to increase the adsorption amount of dye molecules, multilayered mesoporous TiO<sub>2</sub> films have been synthesized by a layer-by-layer deposition. Enhancement of photovoltaic conversion efficiency has been achieved by fabricating multilayered mesoporous TiO<sub>2</sub> photoelectrodes by repeating the cycles of deposition-aging-calcination process . Gratzel's group prepared one micro metre thick mesoporous TiO<sub>2</sub> films by the stacking of three layers. No significant structural perturbation occurred in their mesoporous structure, and the individual layers were tightly adhered. After sensitized by N945 dye, the films yielded a photovoltaic conversion efficiency of 4.04%, about 50% higher than that of traditional films of the same thickness made from randomly oriented anatase nanocrystals.

The photovoltaic conversion efficiency can be further improved by increasing the layers of mesoporous TiO<sub>2</sub> films. However, the mesostructural shrinkage should be taken into account. Prochazka et al. investigated the structural changes for the multilayered mesoporous TiO<sub>2</sub>



films during thermal treatment. They found that the specific surface area and roughness factor of the calcined mesoporous TiO<sub>2</sub> films were not further increased after the deposition of more than 3–5 layers. The new surface area added by deposition of the top layer was compensated by the reduction of the surface area due to the sintering of the bottom layers. The serious limitations in multilayered mesoporous TiO<sub>2</sub> films were also clarified by Huang's group. They prepared multilayered mesoporous TiO<sub>2</sub> films with a thickness up to 4 micro metre on the FTO substrates. The optimal film thickness was proved to be 2.5 micro metres, with photovoltaic conversion efficiency of 5.31%. Bein's group employed the crystallized TiO<sub>2</sub> nanoparticles and the sol-gel Ti-species as NBB in order to construct highly porous and crystallized mesoporous TiO<sub>2</sub> coatings at mild conditions. The beneficial combination of crystallinity and porosity led to greatly enhanced activity of the films in DSSC. The films of only 2.7 micro metre thickness exhibited a conversion efficiency of 6.0%.

Although it is available to construction of DSSC with high photovoltaic conversion efficiency, layer-by-layer deposition is a time-consuming procedure and inevitably increases the fabrication cost of DSSC. A difficult challenge still remains in developing facile synthesis methods to improve the thickness of the highly organized mesoporous TiO<sub>2</sub> films up to several micrometers, an essential dimension for high-efficiency DSSC.

**2.20 Summary-** Due to their well-defined mesopore-wall structure for fast charge carrier transport, and large surface area for more molecular adsorption, highly organized mesoporous TiO<sub>2</sub> films with enhanced photochemical and electrochemical properties offer great opportunities in applications such as photo-catalysis, DSSC, catalytic chemical synthesis, energy storage, drug delivery and others. Considerable challenges still remain in developing high-quality mesoporous TiO<sub>2</sub> films with a thickness up to several micrometers in order to realize the practical applications in photoelectronic devices. The mesoporous structure is easily collapsed once the thickness of the mesoporous TiO<sub>2</sub> films reaches a critical dimension.

Besides, the package density of most currently developed mesoporous TiO<sub>2</sub> films is quite low as compared to that of mesoporous TiO<sub>2</sub> spheres consisting of close-packed nanocrystallines. As a result, the dye adsorption and photovoltaic conversion efficiency are limited. Effects of the textural parameters in mesoporous TiO<sub>2</sub> films, especially wall thickness, pore-size, and pore volume, on the performances of the fabricated devices of DSSC should be well established. [73]

## **2.21 Background leading to the present work.**

### ***Importance of Titanium dioxide films in dye-sensitized solar cells (DSSCs)***

TiO<sub>2</sub> films are used as photo-anodes in DSSCs, owing to their high specific surface area, continuous and tuneable mesoporous structure, and interconnected TiO<sub>2</sub> skeleton with regular nanocrystalline junctions [52, 53]. The film prepared through layer-by-layer deposition showed a highly ordered cubical mesoporous structure [48]. Photo-conversion efficiencies up to 5.35% have been reported.

### ***2.22 Effects of Pre-curing temperature on the film***

Pre-curing temperature in fabrication of the mesoporous film effect the crystallinity, surface area and film adhesiveness to substrate. Thereby it significantly affects the open circuit voltage and short circuit current, thus having importance for influencing the efficiency of DSSCs.

### ***2.23 Effects on efficiency of DSSC***

Improved crystallinity and adhesiveness of the film enhances open circuit voltage and electron transport across the film-substrate interface respectively which is highly desirable for achieving higher photo-conversion efficiency in dye sensitised solar cells.

#### ***2.24 Limitations of varying Pre-curing Temperature***

While lower pre-curing temperature (200°C) is beneficial in preserving the mesoporous structure, but it causes poor adhesiveness of the film to the glass substrate. Whereas, a higher pre-curing temperature (350°C) although promotes crystallinity of the film, but causes shrinkage and collapse of mesopores and is thereby detrimental to mesoporous structure. Thus too low (200°C) or too high (350°C) a temperature results in reduction of DSSCs efficiency due to poor adhesives or lesser surface area of the film as the case may be.

#### ***2.25 Modified Method of varying pre-curing temperature***

The layer- by- layer deposition method of synthesizing TiO<sub>2</sub> films, offers possibility of varying the temperature, in-between the initial coating cycles and subsequent coating cycles. Thus we can attempt to raise pre-curing temperature to higher value (250°C) during initial coating cycle, to achieve adhesiveness of the film to the glass substrate and then reduce the pre-curing temperature to lower value (225°C) during subsequent coating cycles to prevent degradation of mesoporous structure of the film.

#### ***2.26 Advantages of modified pre-curing temperature variation***

The proposed process of changing the pre-curing temperature in-between the coating cycles seems favourable for preserving the both film crystallinity and adhesiveness. The process may thus combine the merits of the both higher and lower pre-curing temperatures, optimally.

#### ***2.27 Aim and scope of the present work:***

1. Synthesis of mesoporous titanium dioxide films using via sol-gel method and layer-by-layer deposition onto a tin oxide coated glass substrate.
2. Fabrication of different sets of films under varying pre-curing temperatures between 200-300°C.

3. Attempting a modified method of varying pre-curing temperature in order to preserve firm adhesiveness of the film to the substrate, even at lower pre-curing temperatures below 250°C.
4. To study the influence of varying pre-curing temperature on:
  - (i) Surface morphology of the TiO<sub>2</sub> films;
  - (ii) Adhesiveness of the TiO<sub>2</sub> film onto the glass substrate
  - (iii) Crystallinity and mesoporous structure of the TiO<sub>2</sub> film
  - (iv) Transmittance spectra of films
  - (v) Absorbance of TiO<sub>2</sub> films with increasing thicknessUsing AFM , SEM and UV-Vis Spectrophotometer.
5. Integration of the synthesised mesoporous titanium dioxide films, as photo-anode, into dye- sensitized solar cells modules.
6. Evaluation of influence of different pre-curing temperature protocols on photo conversion efficiency of the dye-sensitized solar cells.

## Chapter 3

### MATERIALS AND METHODS

**3.1 Chemicals used**-The details of the chemicals used for the synthesis of the mesoporous titanium dioxide films are as given below in the table 3.1. All the chemicals were used as received.

**Table 3.1-** Chemicals used for synthesis of titanium dioxide films

S. No	Name of chemical	Assay	Molecular Weight	Source	LR/AR
1.	Titanium (IV) Isopropoxide	98%	284.26 g/mol	AVRA Synthesis Pvt Ltd, Hyderabad	LR
2.	Ethanol	99.9%	46.08 g/mol	Changshu Yang Yuan chemical, China	AR
3.	De-ionised water	-	18 g/mol	Millipore, IIT Roorke	AR
4.	Acetyl acetone	99%	102.12 g/mol	Sigma Aldrich	LR
5.	Hydrochloric Acid	35.4%	36.46 g/mol	Sd Fine Chem Lab ,Mumbai	AR
6.	Tri-block co-polymer(F-127)	98%	12,600 g/mol	Sigma Aldrich	AR

**3.2 Materials used:** The following lab materials were used in the synthesis of titanium dioxide films.

***List of Materials used and their specifications:***

- 1) Pipettes and Micropipettes- 100,200 and1000 microliters, 5ml, 10ml.
- 2) Beakers (Borosil-25 ml, 50 ml, 100ml
- 3) Micro filter-0.45 micrometer
- 4) Glass rod stirrer
- 5) Conducting Glass Substrate –Fluorine doped tin oxide, type TEC-15(15 Ohm/cm<sup>2</sup>), two in number used per module of solar cell, obtained from Wisconsin University,USA

**3.3 Equipments used:** The following instruments and equipments were used in the process of titanium dioxide films preparation.

***List of Equipments used:***

- 1) Magnetic stirrer-Tarsons Digital Spinot make-MC-2 model
- 2) Weighing Machine- Sartorius Make –BT 224S model
- 3) Spin Coating Machine-APT GmbH automation and Productstecnik make, Spin-150 model
- 4) Spirit Level-For levelling the spin coating machine
- 5) Ceramic Top Hot Plate (Upto 500 degree Celsius)- Tarsons Digital Spinot -MC-2 model
- 6) Heating Furnace (Temperature ramp rate 1 degree/minute)-Lenton, England, UAF15/5
- 7) Digital multimeter- Two in number (having micro ampere and micro volts range scale)

**3.4 Test Equipment:** The below mentioned test equipments were used for studying the properties of the prepared titanium dioxide films.

***List of Test Equipments used:***

- 1) Atomic Force Microscope – G-20 TECHNAI, Netherland
- 2) Scanning Electron Microscope-Quanta 200 F, FEI, Netherland
- 3) X-Ray Diffractometer- D 8 Advance (Cu K $\alpha$  ) Bruker ,Germany
- 4) UV-Vis Spectrophotometer-VARIAN 5000 Uv-Vis-NIR

---

**4.1-Preperation of solution for mesoporous  $TiO_2$  Film-** A precursor solution was first prepared by mixing appropriate amounts of ethanol (99.9%), hydrochloric acid (HCl, 35.4%), titanium tetra isopropoxide (TTIP,98%), acetyl acetone (AcAc, 99 %), and deionised water ( $H_2O$ ), and followed by stirring for two hours. Tri-block copolymer Pluronic F127 (EO106PO70EO106) was dissolved in ethanol and then mixed with the precursor solution. Molar ratios of these ingredients were maintained as follows: TTIP/AcAc/HCl/ $H_2O$ /Ethanol/F127=1:0.5:0.5:15:40:0.004.



**Figure4.1-Showing magnetic stirring process of the solution**

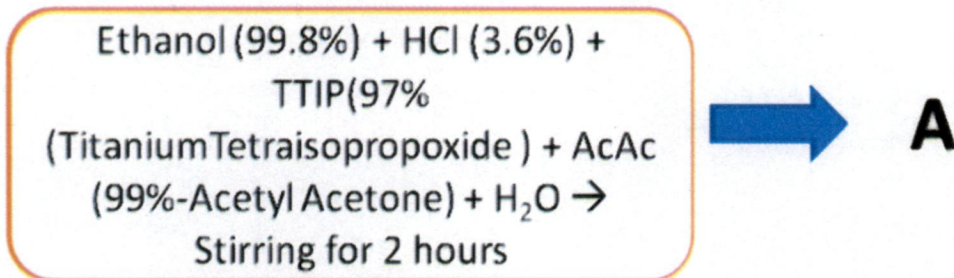
The solution was kept on magnetic stirrer for three hours more to get a homogeneous mixture. The beaker containing the solution was covered with aluminium foil to protect against atmospheric contamination. The beaker needs to be kept precisely centred to prevent the magnetic bead touching the beaker surface edges which can cause wear off of the bead.



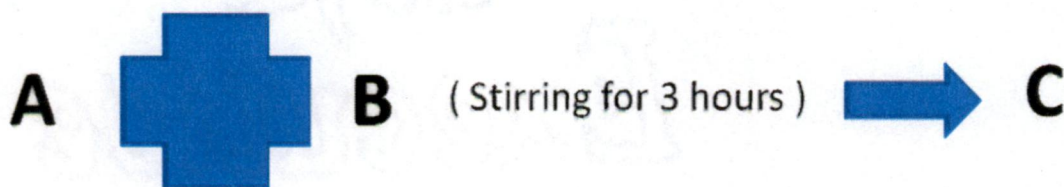
The process of making the initial solution is pictorially depicted below.

## Method of preparation of film

Precursor solution:



**B** - F127 (Triblock co-polymer pluronic – in Ethanol)



**4.2: Filtering of solution** - After stirring for three hours more, the sol solution thus obtained was filtered using 0.45micron filter ( shown below in figure 4.2) to filter out the possible atmospheric contaminants and the particles mixed due to wear off of the magnetic bead. Then the solution was taken into syringe associated with the spin-coater.



**Figure4.2-Showing the 0.45 micron filter**



**4.3:Spin coating**-After stirring for three hours more, the sol solution thus obtained was deposited on the fluorine-doped tin oxide (FTO, TEC 15 from Harford Glass company,USA) 3 mm thick, 80% transmittance in the visible, 15  $\Omega$ /sq) substrates by spin coating (2000 rpm for 1 min) at a relative humidity of about 70%.



**Figure 4.3**-showing the testing of the FTO glass substrate

It is utmost essential to check that the spin coating is done on the conducting side of the FTO glass. The conducting side of the FTO was identified using digital millimetre as shown above in figure. The meter usually shows 15 -20 ohms when leads are kept one cm apart on the conducting side, while the non -conducting side will show very-very high resistance.

Also it is necessary to thoroughly clean the glass substrate using ultra sonicator to remove all contaminants from the surface to be coated. The glass need to be dried fully and cleaned with acetone.

To protect a small portion on one edge of the glass from getting spin- coated it was covered with a thin layer of plaster of Paris. Many other methods reported earlier were tried but proved inadequate. Some allowed seepage while others left adhesive residues on the glass.non conducting side of the glass can be marked by identification number of the sample using marker pen. Also follow alternate means of having identification marks on the samples since

pen markers' ink gets erased due to ethanol treatment and also due to heating during the pre-curing process.



**Figure4.4- showing the spin coating machine used.**

The spin coating machine needs to be balanced on the floor surface using spirit level to ensure even spread of the solution on the glass substrate, otherwise the liquid drops will flow towards the lower ends of the machine. The vacuum pump needs to be placed far away or on a separate platform so that the floor surface is free from vibrations of the vacuum pump

**4.4 Ethanol treatment** - The spin-coated film was exposed to ethanol vapour for 5 min at room temperature by dropping liquid ethanol on a filter paper surrounding the sample enclosed in a Petridis as shown below in figure 4.5.



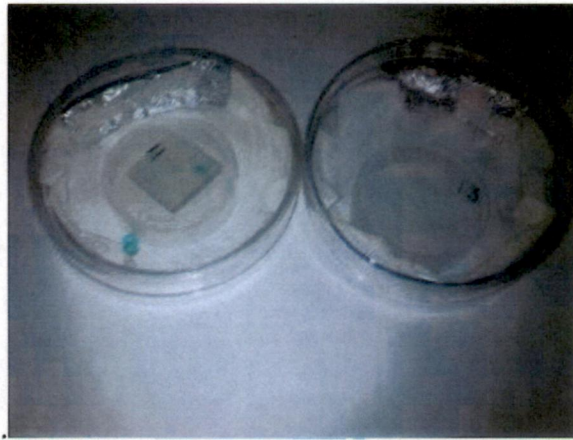


**Figure 4.5-showing the step of ethanol vapour treatment**

. The vapour treatment reduces the surface irregularity and lessens the strain in the film by slowing down the drying process.

**4.5-Pre-curing:** The film was then pre-cured on a hot plate at certain temperature (200-300°C) for 15 min in air to enhance the inorganic polymerization and to stabilize the mesophases involved. The ceramic top hotplate used is shown below in figure 4.6.

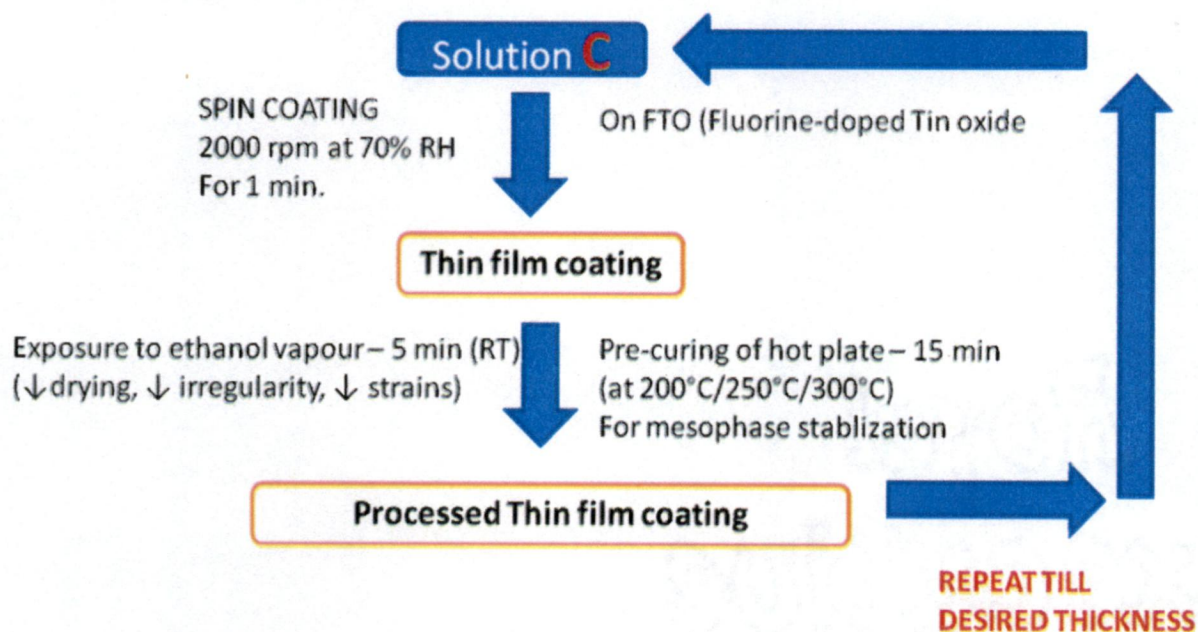


**Figure 4.6-shows the step of pre-curing on the hot plate**

Repetitive spin-coatings, exposing to ethanol vapour, and pre-curing were carried out as depicted pictorially below, until the desired film thickness was reached.

# Method of preparation of film cont.

- Solution C used for spin coating:

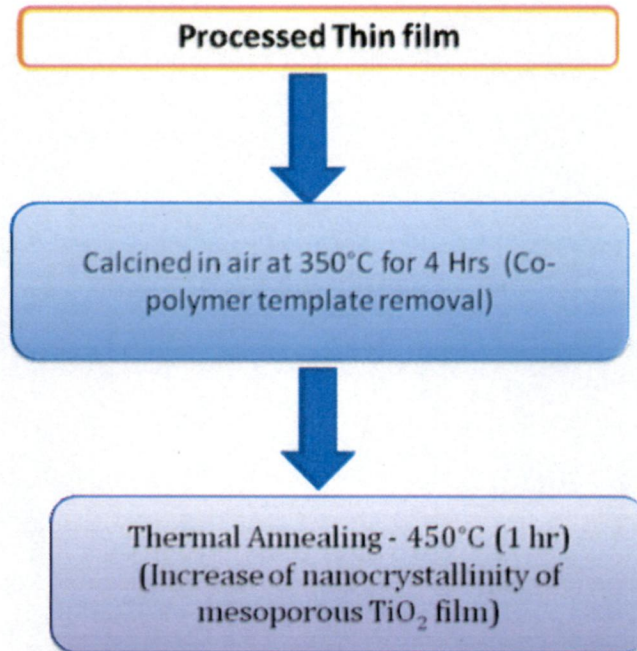


**4.6-Heat treatment:** Thereafter, the film sample was calcinated in air at 350 °C for 4 hours (1 °C/min ramp) to completely remove the organic copolymer templates .Finally the film was thermally annealed at 450 °C for 1 hour (1 °C/min ramp) to improve the nanocrystallinity of the mesoporous TiO<sub>2</sub>.The process flow diagram is shown below.



# Method of preparation of film cont.

- Post processing of film:



The programmable furnace employed for calcinations/ annealing is shown below in figure 4.7



**Figure4.7-Shows the programmable furnace used for calcinations/annealing**

**4.7-Overall process flow:** The overall process followed for the film preparation is diagrammatically summarised below.

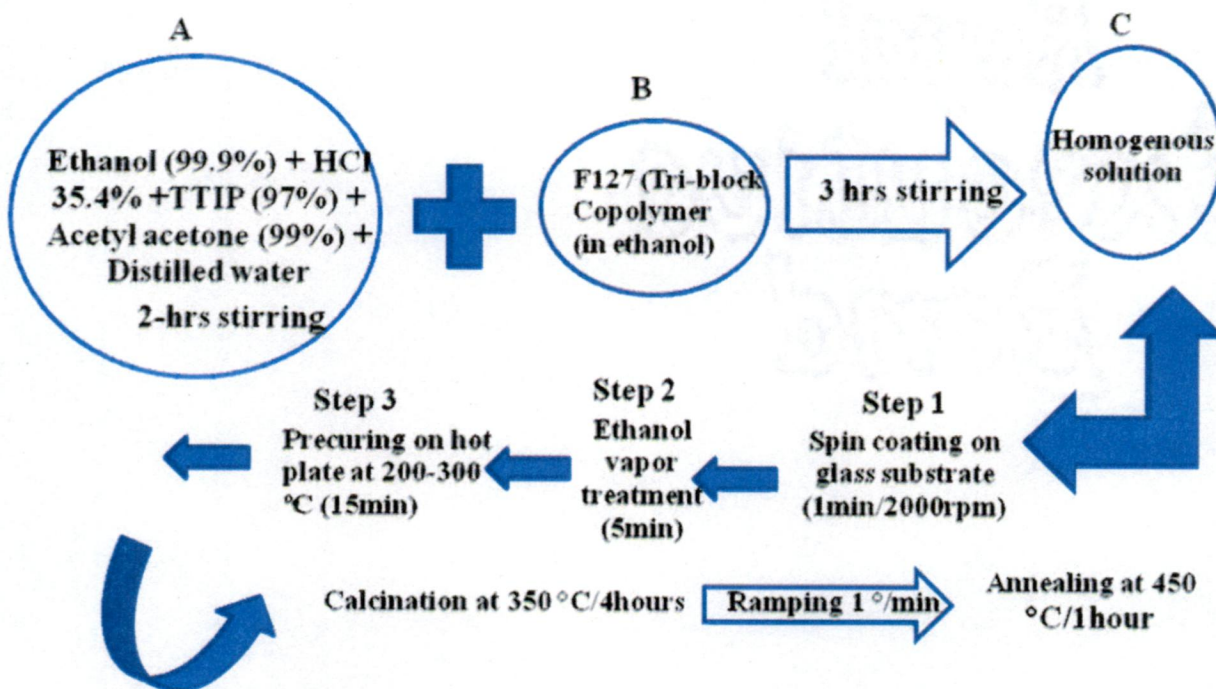


**Figure 4.1: Schematic representation of procedure followed for TiO<sub>2</sub> film preparation.**

**4.8-Cooling and storage-** After annealing the films were allowed to cool down in air and then stored in moisture- free air sealed boxes (containing silica-gel pouches), to protect against environmental degradation and atmospheric contamination.

**4.9-Precautions and safety measures:** The glass containers must be thoroughly cleaned and dried before use to prevent impurities. Titanium tetra isopropoxide must be handled very carefully as it is highly sensitive to moisture and vapours rapidly above 15 degree Celsius. The solution should be kept covered throughout the process to prevent contamination. Uninterrupted power supply should be ensured at the start of the experiment since any break in the process will severely affect the results and may even complete failure to achieve desired results. The FTO glass substrate should be thoroughly cleaned before coating. Use face mask and protective hand gloves for personnel safety against possible inhalation of TiO<sub>2</sub> fumes,

which are heavier than air, and tend to settle down in the vicinity. Exhaust fan may be used to ventilate the working area. The process protocol should be strictly adhered to since even a very minute variation in process parameter like humidity aging, temperature protocol, temperature ramping rate can alter the results drastically.

#### **4.10: Preparation of cell modules:**

1. Allow the films slide to cool to room temperature.
2. Place the slide face down in the Petridis containing dye.
3. Allow it to soak the dye for 12 hours.
4. Coat the second slide with gold using sputtering (30 nm thick).
5. After TiO<sub>2</sub> slide have adsorbed dye, remove and rinse with ethanol and blot dry.
6. Place the two slides over each other in a slightly offset manner.
7. Bind them together with binder clips.
7. One drop liquid iodide solution is then added between the slides.
8. Capillary action will stain the entire slide.
9. Place the conducting copper tape on the exposed portion of the conductive side.
10. Solder wire connection on each slide on the copper tape.
11. Carry out I-V measurements and calculate efficiency using formula given bellow:

$$\text{Efficiency} = (\text{Voc} \times \text{Isc} \times \text{FF}) / \text{Incident Radiation}$$

Where Voc- Open circuit voltage (in volts)

Isc- Short circuit current density (milli- amperes / sq cm)

FF-fill factor= (On load max current × On load max voltage) / (Voc× Isc)

Incident radiation-100 milliwatts /sq cm, at Air mass- 1.5

#### ***4.11-Characterization***

The efficiency of DSSCs is highly dependent upon the particle size of TiO<sub>2</sub> film, surface morphology and porosity of the film.

***4.111-X-Ray diffraction***-X-Ray diffraction measurements were carried out to identify crystalline phase and crystallinity of TiO<sub>2</sub> present in the mesoporous films using X-Ray Diffractometer- D8- Advance, Bruker- axs, Germany .

***4.112- Atomic force micrography*** : Atomic force micrography was performed to study surface morphology and structure of the films using Atomic Force Microscope FEI, Netherland.

***4.113-Scanning Electron Micrographs***: Scanning Electron Micrographs were obtained to observe the adhesiveness of the film onto the glass substrate using Scanning Electron Microscope-Quanta 200 F, FEI, Netherland.

***4.114-Transmittance /Absorbance***: Transmittance and absorbance characteristics were studied using UV-Vis Spectrophotometer 200 F, FEI, Netherland -VARIAN 5000Uv-Vis-NIR.



**5.1 Atomic force microscopy (AFM):** AFM was performed to study surface morphology and structure of the films using Atomic Force Microscope FEI; Netherland.

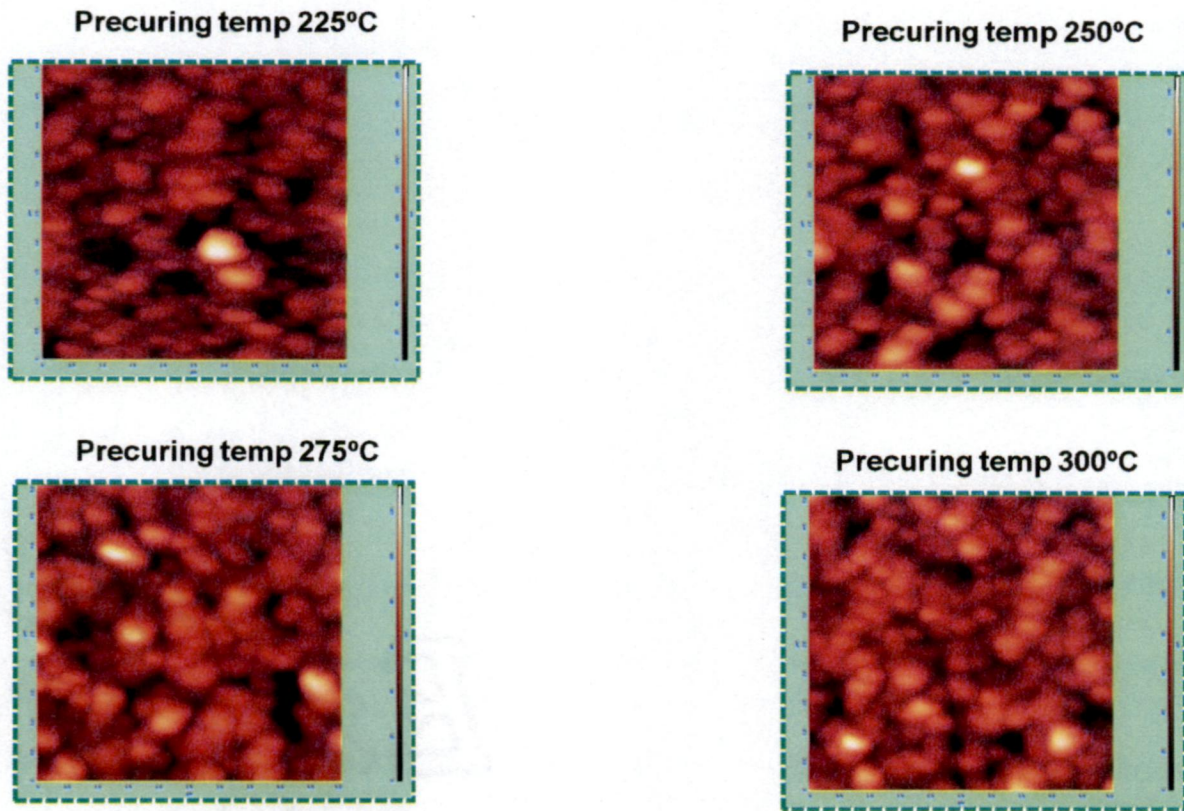


**Figure5.1-** Figures depicting the atomic force micrographs (2-D view) of TiO<sub>2</sub> film, at pre-curing temperature 225, 250, 275 and 300°C as shown on the top of each micrograph.

The (2-diamentional view) micrographs obtained for the films prepared under different pre-curing temperatures shown in figure 5.1 above.



The micrograph demonstrates the presence of nanoscale pits in the  $\text{TiO}_2$  islands. The 2-dimensional view micrographs of the films is exhibiting a highly ordered well connected porous network with uniform nanocrystalline structures. The nanocrystalline  $\text{TiO}_2$  particles are seen as bright structures while the pores are seen as dark hollow pits. The crystallinity is observed to be enhancing whereas the mesopores are degrading with the rise in pre-curing temperature. This may be due to promotion of nuclei formation at higher pre-curing temperatures, thus promoting crystallinity which is in agreement with the reported results.

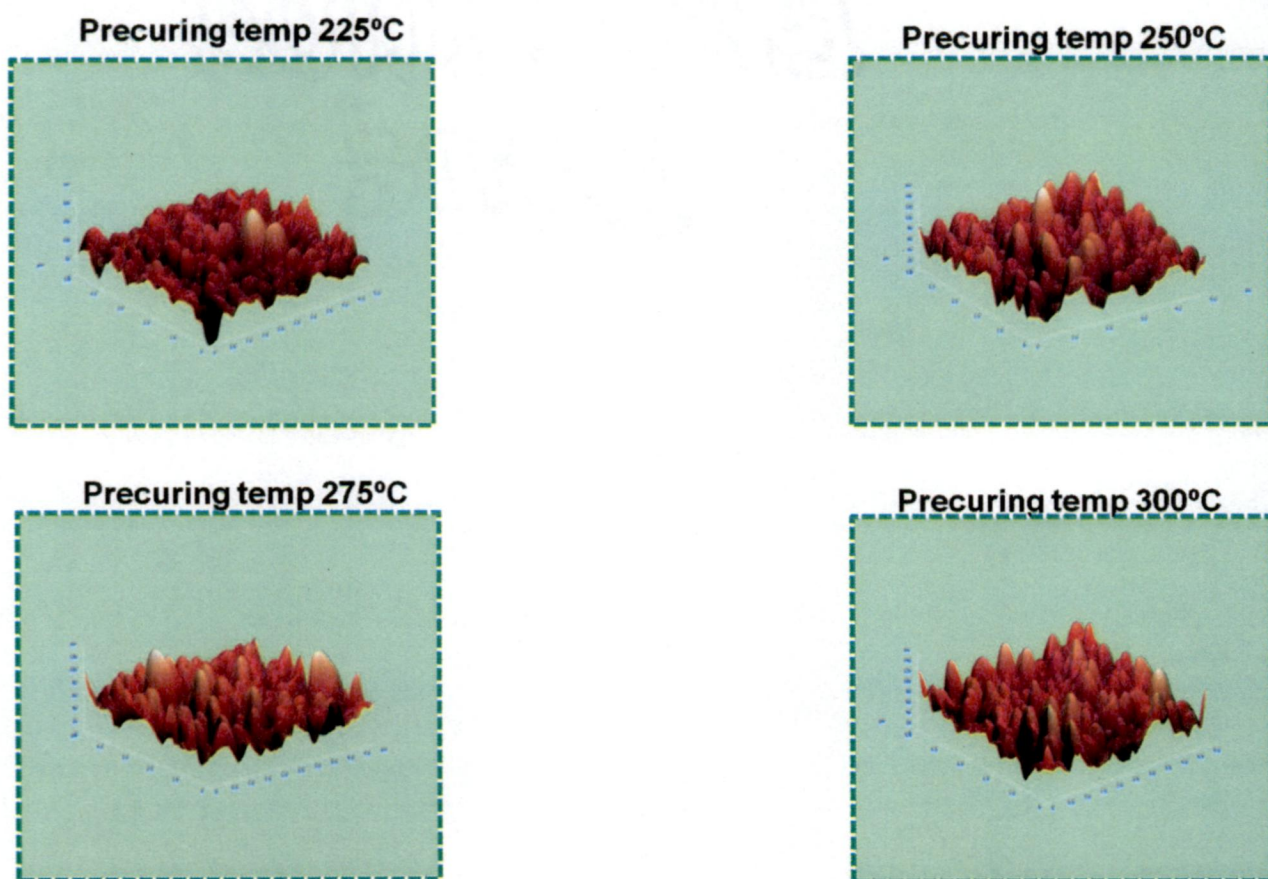


**Figure 5.2-** Figures depicting the atomic force micrographs (3-D view) of  $\text{TiO}_2$  film, pre-curing at a temperature of 225, 250, 275 and 300°C as shown on the top of each micrograph.

Roughness shows a slight change, ranging between 18 nm-26 nm but it does not seem to follow any trend while particle size varied between 66 nm-114 nm with size being more uniform at higher temperatures, with respect to pre-curing temperature variation from 225-300 degree Celsius. The as prepared films are seen to be homogeneous and porous with a

narrow size distribution of particles. These microstructural characteristics (porosity and particle size) determine the degree of dye adsorption.

**5.2 -X-Ray diffraction (XRD):** Following are the X-Ray diffraction patterns obtained for the titanium dioxide films pre-cured at different temperatures ranging from 225 degree Celsius to 300 degree Celsius.

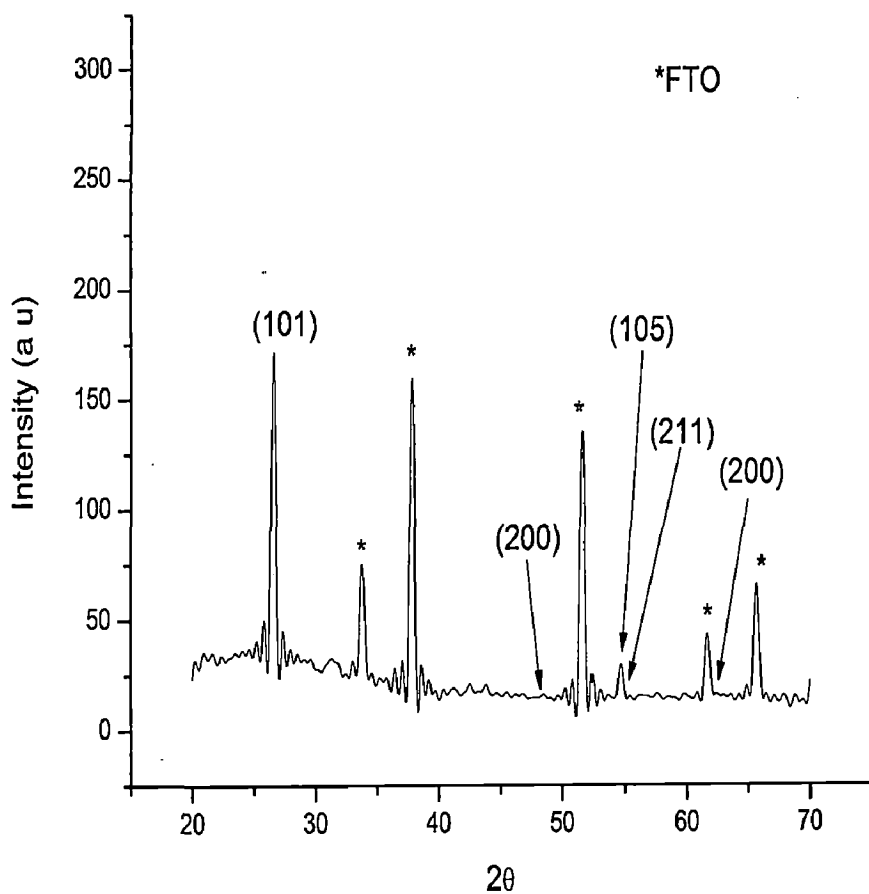


**Figure -5.3- XRD spectra of TiO<sub>2</sub> film pre-cured at 275°C**

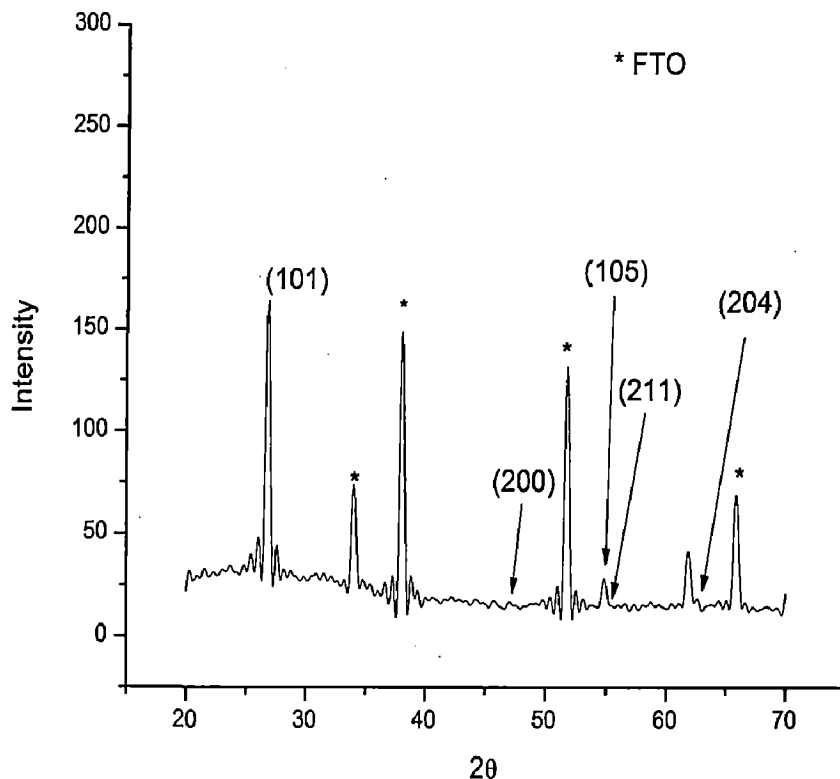


**Figure 5.4- XRD spectra of TiO<sub>2</sub> film pre-cured at 300°C**

The Titanium dioxide films were prepared by co-block polymer templating via sol-gel method and then spin coated onto Fluorine doped tin oxide (FTO) glass substrate. Structural characterisation of the coated films was performed using X-Ray diffractometer (Copper K - alpha radiation). The high intensity of XRD peaks shows that the film layers exhibit a high crystallinity. The peaks in the XRD pattern can be ascribed to (101), (200), (105), (211), and (204) planes of titanium dioxide anatase phase respectively. The star marked peaks in the XRD pattern correspond to the constituents present in the glass substrate (FTO). The peaks in the XRD pattern were observed to be in conformity with the previously reported results [51]. The difference observed was that the peaks from plane (105) and (211) were sharper in our results as compared to slightly broader peaks in works reported. Also the smaller peaks became more pronounced on higher pre-curing temperature (300°C) than at lower temperature (225°C) which is due to promotion of nucleation with rising temperature.

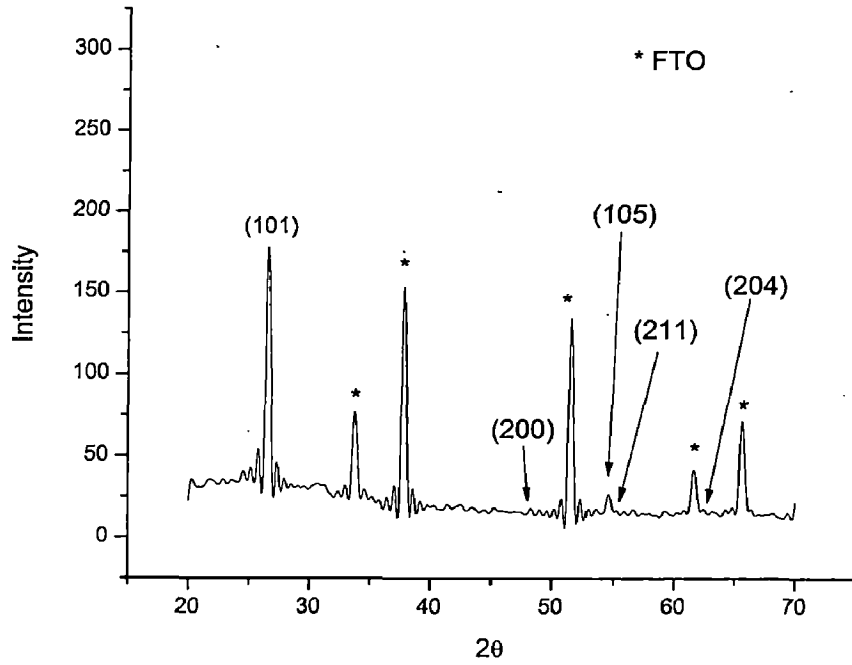


**Figure 5.5- XRD spectra of TiO<sub>2</sub> film pre-cured at 250°C**

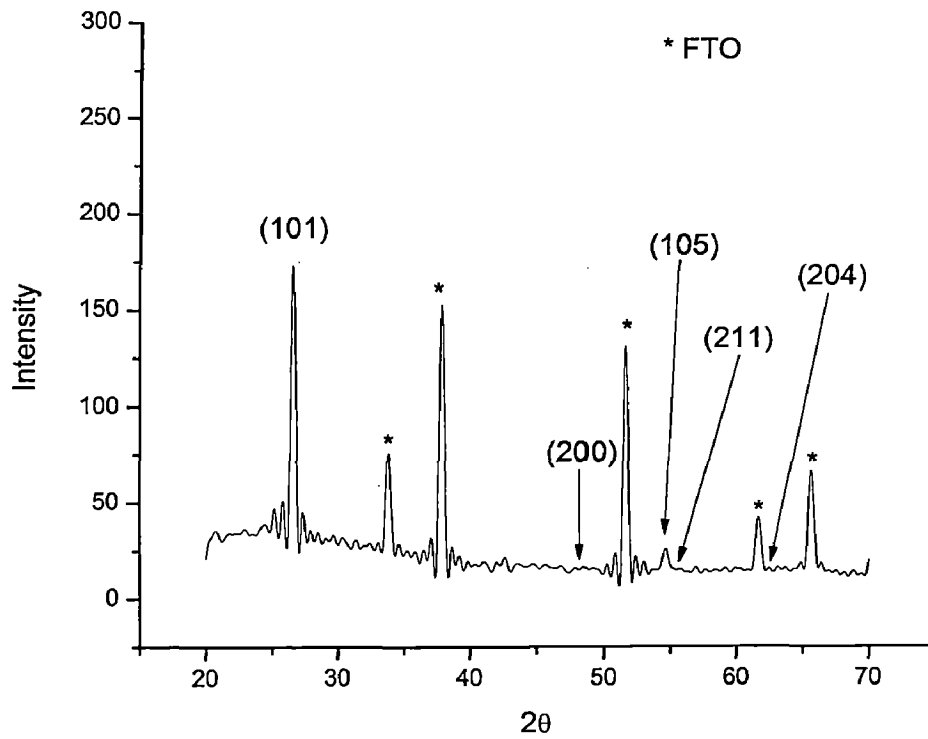


**Figure 5.6- XRD spectra of TiO<sub>2</sub> film pre-cured at 225°C**

**5.3. Scanning electron microscopy (SEM):** Scanning electron microscopy was carried out in order to characterize film layers and adhesion of first layer to the substrate, pre-cured under different temperature regimes.

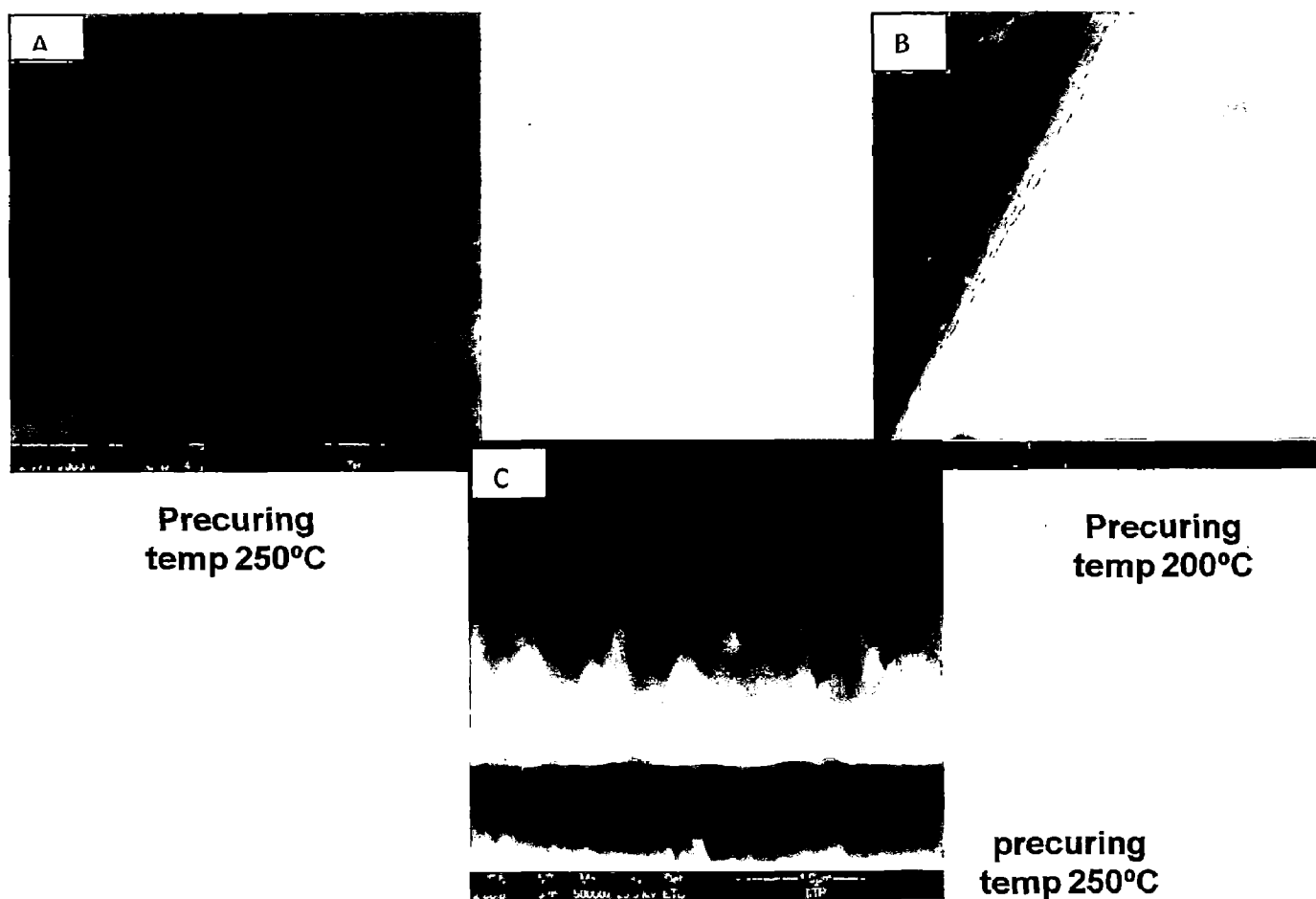


**Fig 5.7 A, B and C depicting the Scanning electron micrograph (Cross-sectional) of TiO<sub>2</sub> film. Fig 4.5 A evinced multilayer coating of TiO<sub>2</sub> at 250° Fig 4.5B showing distorted monolayer of TiO<sub>2</sub> at 200°C pre-curing temperature and Fig. 4.5 C showing firm adhesion of TiO<sub>2</sub> film with substrate at pre-curing temperature of 250°C**

The film pre-cured at a temperature of 200 degrees Celsius was observed to have developed cracks and seems to be peeling off from the substrate as seen in FE-SEM micrograph in figure B above.

Whereas, the film prepared by employing modified pre-curing temperature protocol, that is by having the first layer pre-cured at 250 degrees Celsius and then lowering the temperature to coat the subsequent layers of the film (seen in figure C) above were observed to be firmly adhering to the substrate Figure A above is showing cross-sectional FE- SEM view of the uniform multi-layers of the films coated on the FTO glass substrate. The modified pre-curing temperature method adopted here is advantageous in preserving the adhesiveness of the film layer to the glass substrate and simultaneously allowing us to prevent damage of mesopores due to higher pre-curing temperature.

It has been possible to attain good adhesiveness with the as applied pre-curing temperature protocol, because layer- to-layer stress in the film is lesser than the stress between the first film layer and the glass substrate. The modified temperature protocol seems effective for preserving both adhesiveness of the film coating onto the glass substrate and evenness and porosity of the subsequent film coatings even at lower temperature.



**5.4. UV-Vis Spectroscopy:** UV-Vis Spectrophotometry was carried out to ascertain the influence of variation in pre-curing temperature on transmittance spectra of the films. Transmission spectra revealed a definite change with respect to temperature, as temperature increased from 225 to 250°C there is significant increase in the transmittance. Absorbance enhances due to the decreased reflectivity offered to the incident light, which translates into increased transmittance. However further increase in temperature leads to saturation in the transmittance. This is attributed to the morphological changes occurring with change in temperature

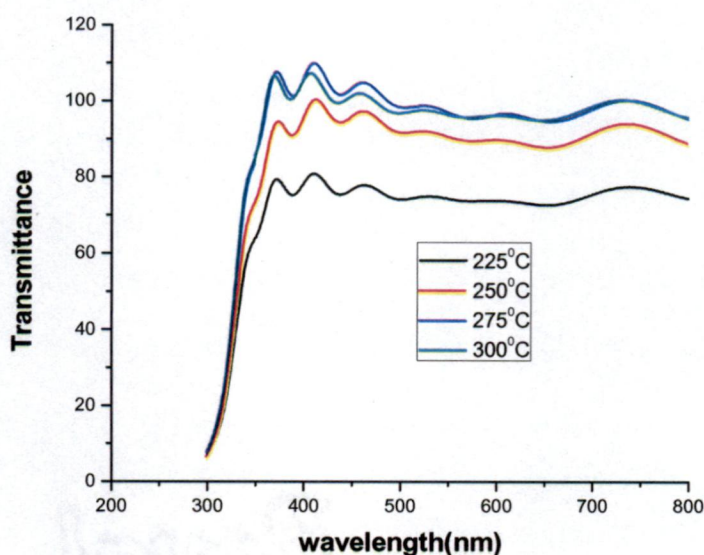


**Fig 5.8- UV-Vis Spectrophotometry showing, influence of increasing pre-curing temperature on transmittance of the films.**



**5.5 UV-Vis Spectrophotometry-** UV-Vis Spectrophotometry was carried out to ascertain influence of increasing film thickness on absorbance of the films. Absorbance spectra revealed a linear increase in absorbance on increasing the number of thin film layers which is attributed to increased uptake of dye by virtue of increase in total surface available for the attachment of the dye onto the TiO<sub>2</sub> film.

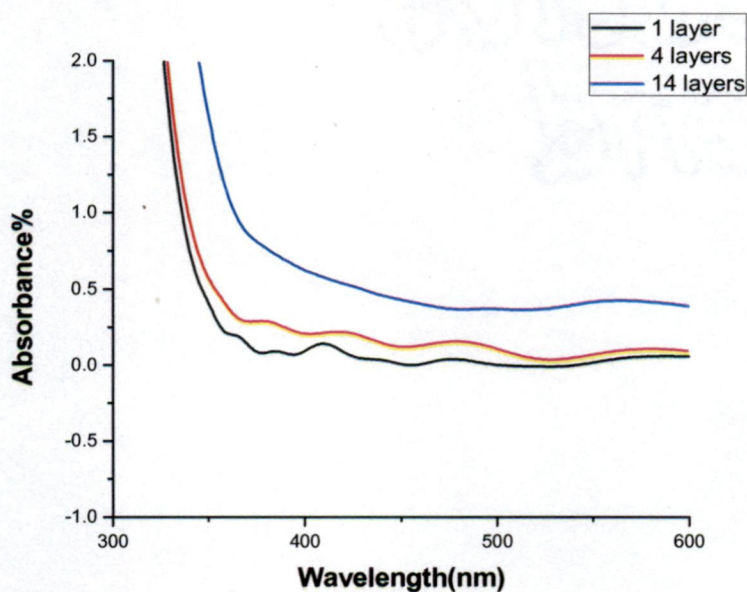


**Fig 5.9 UV-Vis Spectrophotometry showing rise in absorbance with increasing film layers**

**5.6 Thickness measurement using Surface Profilometer-** Average film thickness of monolayer measured by using surface profilometer was 220 nm. This is necessary in order to obtain a film of the desired thickness to be integrated into the DSSCs for optimum efficiency and also to ascertain that the coating is uniform all over the surface. The Profilometer graph shows uniform thickness coated film layer.

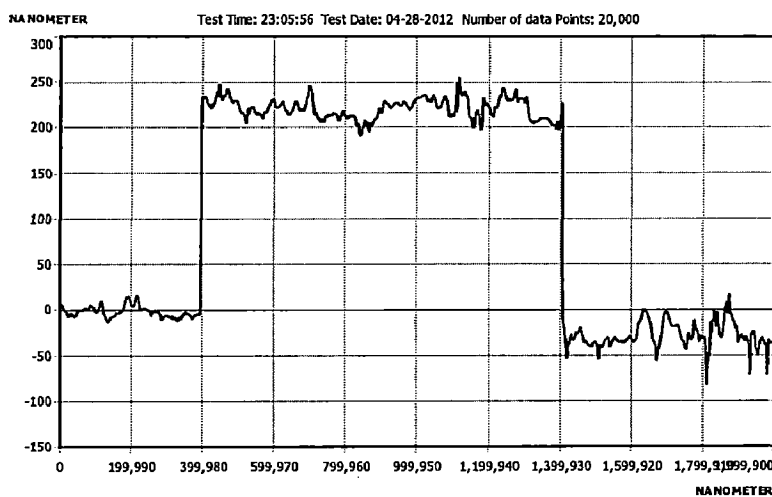


**Figure.5.10. Showing thickness of uniform monolayer of coated film**

### 5 Evaluation of DSSCs Efficiency –

The photo-conversion efficiency measurement was carried out using formulae given below:

$$\text{Efficiency} = (\text{Voc} \times \text{Isc} \times \text{FF}) / \text{Incident Radiation}$$

Where Voc- Open circuit voltage (in volts)

Isc- Short circuit current density (milli- amperes / sq cm)

FF-fill factor= (On load max current × On load max voltage) / (Voc× Isc)

Incident radiation-100 milliwatts /sq cm, at Air mass- 1.5

The open circuit voltage, short circuit current, fill factor and finally the photo-conversion efficiency was calculated for the as prepared DSSCs), to study the influence of change in pre-curing temperature on the efficiency of the cells, as shown in the table below.

**Table 5.1-Photovoltaic performance of DSSCs at varying pre-curing temperatures**

Temperature (degree Celsius)	Short-circuit current( $\mu\text{A}/\text{cm}$ )	Open circuit voltage(volts)	Fill Factor (%)	Efficiency (%)
225	185	0.497	53	0.049
250	236	0.529	58	0.072
275	245	0.522	62	0.079
300	215	0.510	59	0.065

The efficiency is seen to be increasing with rise in the pre-curing temperature from 225 to 275 degree Celsius and decreases above 275 owing to fall in short circuit current. The increase in efficiency can be ascribed to the increase in crystallinity with the rise in temperature due to enhanced nucleation. Whereas, as the temperature is raised further the damage caused to the mesoporous structure predominates the benefits obtained by increased crystallinity. Thus the efficiency seems to be maximising at 275 degree Celsius.

The current- voltage curves for DSSCs fabricated using photoanodes prepared at varying pre-curing temperatures are shown below.

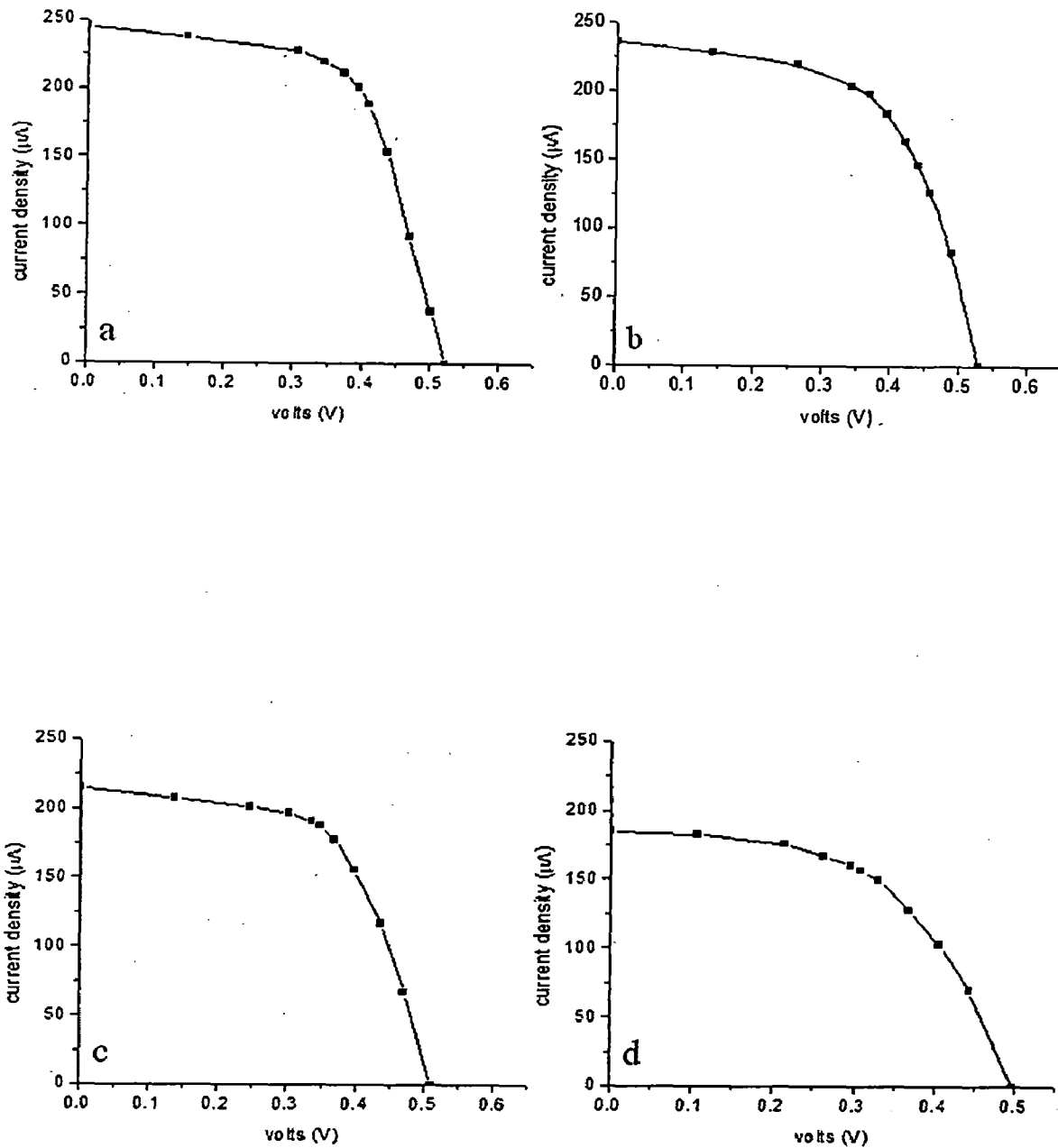


**Fig-5.11- Current-voltage curves for films pre-cured at a) 250°C b) 275°C c) 300°C and d) 225°C.**

## Chapter 6 CONCLUSIONS

---

Highly crystalline and ordered mesoporous TiO<sub>2</sub> films were prepared with different pre-curing temperature and varied thickness using block polymer templating sol-gel route combined with layer- by- layer deposition method.

Pre-curing temperature evinced significant effect on film morphology as observed by AFM. Films shows loose attachments and structural damages at 200°C and to overcome this problem, a modified pre-curing temperature regime was adopted to get firm adhesiveness of the film on to the substrate even at low temperature (below 250°C) which was confirmed by Scanning Electron Microscopic examination.

UV-Visible spectroscopic examination suggests thickness dependent increase in absorbance. As number of layers increase, absorbance also increases linearly. This is attributed to the increased uptake adsorption of the dye by additional surface area of subsequent film layers. Further, transmittance study revealed pre-curing temperature dependent change in transmittance of film. Initially there was increase in transmittance, when temperature increased from 225 to 275°C. Beyond this, no significant change in transmittance was observed. As pre-curing temperature was raised beyond 275°C the transmittance get saturated.

The efficiency of cell modules fabricated using as synthesized TiO<sub>2</sub> films shows increase in the efficiency with rise in the pre-curing temperature from 225 to 275 degree Celsius and decreases above 275 owing to fall in short circuit current. The increase in efficiency can be ascribed to increased crystallinity with the rise in temperature. Whereas, a further rise in temperature causing damage to the mesoporous structure, predominates the benefits obtained by increased crystallinity. The efficiency is seen to be maximising at a pre-curing temperature of 275 degree Celsius.

# Conference proceedings:

1. **Harjeet Singh**, Shejale Kiran Prakash, Himanshu Panjiar, B.S.S. Daniel. “Synthesis of mesoporous Titanium dioxide films for Dye Sensitized Solar Cells” **accepted for presentation (and publication review) in International Conference AMPCO 2012** at Indian Institute of Technology Roorkee, Roorkee, India during 2-4 Nov 2012.
2. Shejale Kiran Prakash, Himanshu Panjiar, **Harjeet Singh**, Sanjeev Manhas, B.S.S. Daniel. “Application of graphene oxide and TiO<sub>2</sub> in the fabrication of Solar Cell module by electrodes modification” **accepted for presentation (and publication review) in International Conference AMPCO 2012** at Indian Institute of Technology Roorkee, Roorkee, India during 2-4 Nov 2012.
3. **Conference attended Nanosolar 2012 - International Conference** at Amrita University, Kochi, Kerala during 21-23 Feb 2012.
4. **Attended International conference and workshop** on nanostructured ceramics and other nanomaterials at Delhi University, Delhi during 13-16 March 2012.
5. **Attended short term course** on Off-grid Solar PV Components and Systems, organized in collaboration with IIT-Bombay, at India Habitat Centre, New Delhi during 11-13 April 2012.

## REFERENCES

- [1] B. O'Regan, M. Gratzel, *Nature* 353 (1991) 737.
- [2] MR Narayan , Review: Dye sensitized solar cells based on natural photosensitizers(In press). *Renew Sustain Energy Rev* (2011), doi:10.1016/j.rser.2011.07.148
- [3] M.K. Nazeeruddin, P. Pechy, T. Renouard, S.M. Zakeeruddin, R. Humphry-Baker, P. Comte, P. Liska, P. Liska, L. Cevery, E. Costa, V. Shklover, L. Spiccia, G.B. Deacon, C.A. Bignozzi, M. Gratzel, *J. Am. Chem. Soc.* 123 (2001) 1613.
- [4] M. Adachi, Y. Murata, J. Takao, J. Jiu, M. Sakamoto, F. Wang, *J. Am. Chem. Soc.* 126 (2004) 1613.
- [5] N.G. Park, M.G. Kang, M.K. Kim, K.S. Ryu, S.H. Chang, J. van de Lagemaat, K.D. Benkstein, A.J. Frank, *Langmuir* 20 (2004) 4246.
- [6] H.S. Lung, J.K. Lee, S. Lee, K.S. Hong, H. Shin, *J. Phys. Chem. C* 112 (2008) 8476.
- [7] D. Zhao, T. Peng, L. Lu, P. Cai, P. Jiang, Z. Bian, *J. Phys. Chem. C* 112 (2008) 8486
- [8] A. E. Becquerel, *Comt. Rend. Acad. Sci.* 9, 561 (1839).
- [9] H. Shirakawa, E. J. Louis, A. G. MacDiarmid, C. K. Chiang, A. J. Heeger, *Chem. Commun* 16, 578 (1977).
- [10] O'Regan B, Grätzel M. A low-cost, high-efficiency solar-cell based on dye-sensitized colloidal TiO<sub>2</sub> films. *Nature* 1991; 353:737–40.
- [11] F Kong , S Dai ,K Wang . Review article: review of recent progress in dye-sensitized solar cells. *Advances in OptoElectronics* 2007; 2007: 1–13.
- [12] Y Chiba ,A Islam ,Y Watanabe , R Komiya ,N Koide ,L Han. Dye-sensitized solar cells with conversion efficiency of 11.1%. *Japanese Journal of Applied Physics* 2006; 45:L638–40.
- [13] NJ Cherepy ,GP Smestad , M Grätzel ,JZ Zhang . Ultrafast electron injection: implications for a photoelectrochemical cell utilizing an anthocyanin dye-sensitized TiO<sub>2</sub> nanocrystalline electrode. *Journal of Physical Chemistry* 1997; 101:9342–51.
- [14] GP Smestad . Education and solar conversion: demonstrating electron transfer. *Solar*
- [15] H.J. Snaith, L.S. Mende, *Adv. Mater.* 19 (2007) 3187.
- [16] T.W. Hamann, R.A. Jensen, A.B.F. Martinson, H.V. Ryswyk, J.T. Hupp, *Energy*

Environ. Sci. 1 (2008) 66. 15][17] P.E. de Jongh, D.J. Vanmaekelbergh, Phys. Rev. Lett. 77 (1996) 3427.[18] G. Schlichthörl, S.Y. Huang, J. Sprague, J. Phys. Chem. B 101 (1997) 8141.

[19] G.J.D.A.A. Soler-Illia, C. Sanchez, B. Lebeau, J. Patarin, Chemical strategies to design textured materials: from microporous and mesoporous oxides to nanonetworks and hierarchical structures, Chem. Rev. 102 (2002) 4093–4138.

[20] H.S. Yun, K. Miyazawa, H. Zhou, I. Honma, M. Kuwabara, Synthesis of mesoporous thin TiO<sub>2</sub> films with hexagonal pore structures using triblock copolymer templates, Adv. Mater. 13 (2001) 1377–1380.

[21] Y.K. Hwang, K.C. Lee, Y.U. Kwon, Nanoparticle routes to mesoporous titania thin films, Chem. Commun. (2001) 1738–1739.

[22] D. Grosso, G.J.A.A. De Soler-Illia, F. Babonneau, C. Sanchez, P.A. Albouy, A. Brunet-Bruneau, A.R. Balkenende, Highly organized mesoporous titania thin films showing mono-oriented 2D hexagonal channels, Adv. Mater. 13 (2001) 1085–1090.

[23] E.L. Crepaldi, G.J.d.A.A. Soler-Illia, D. Grosso, F. Cagnol, F. Ribot, C. Sanchez, Controlled formation of highly organized mesoporous titania thin films: from mesostructured hybrids to mesoporous nanoanatase TiO<sub>2</sub>, J. Am. Chem. Soc. 125 (2003) 9770–9786.

[24] P.C.A. Alberius, K.L. Frindell, R.C. Hayward, E.J. Kramer, G.D. Stucky, B.F. Chmelka, General predictive syntheses of cubic, hexagonal, and lamellar silica and titania mesostructured thin films, Chem. Mater. 14 (2002) 3284–3294.

[25] G.J.D.A.A. Soler-Illia, C. Sanchez, B. Lebeau, J. Patarin, Chemical strategies to design textured materials: from microporous and mesoporous oxides to nanonetworks and hierarchical structures, Chem. Rev. 102 (2002) 4093–4138.

[26] E.L. Crepaldi, G.J.d.A.A. Soler-Illia, D. Grosso, F. Cagnol, F. Ribot, C. Sanchez, Controlled formation of highly organized mesoporous titania thin films: from mesostructured hybrids to mesoporous nanoanatase TiO<sub>2</sub>, J. Am. Chem. Soc.



125 (2003) 9770–9786.

[27] D. Grosso, F. Cagnol, G.J.D.A.A. Soler-Illia, E.L. Crepaldi, H. Amenitsch, A. Brunet-Bruneau, A. Bourgeois, C. Sanchez, Fundamentals of mesostructuring through evaporation-induced self-assembly, *Adv. Funct. Mater.* 14 (2004) 309–322.

[28] L.N. Protasova, E.V. Rebrov, T.S. Glazneva, A. Berenguer-Murcia, Z.R. Ismagilov, J.C. Schouten, Control of the thickness of mesoporous titania films for application in multiphase catalytic microreactors, *J. Catal.* 271 (2010) 161–169.

[29] C. Sanchez, C. Boissiere, D. Grosso, C. Laberty, L. Nicole, Design, synthesis, and properties of inorganic and hybrid thin films having periodically organized nanoporosity, *Chem. Mater.* 20 (2008) 682–737.

[30] D. Grosso, G.J.D.A.A. Soler-Illia, E.L. Crepaldi, F. Cagnol, C. Sinturel, A. Bourgeois, A. Brunet-Bruneau, H. Amenitsch, P.A. Albouy, C. Sanchez, Highly porous TiO<sub>2</sub> anatase optical thin films with cubic mesostructure stabilized at 700 °C, *Chem. Mater.* 15 (2003) 4562–4570.

[31] J.H. Pan, D.D. Sun, C. Lee, Y.J. Kim, W.I. Lee, Effect of calcination temperature on the textural properties and photocatalytic activities of highly ordered cubic mesoporous WO<sub>3</sub>/TiO<sub>2</sub> films, *J. Nanosci. Nanotechnol.* 10 (2010) 4747–4751.

[32] J.D. Bass, D. Grosso, C. Boissiere, C. Sanchez, Pyrolysis, crystallization, and sintering of mesostructured titania thin films assessed by in situ thermal ellipsometry, *J. Am. Chem. Soc.* 130 (2008) 7882–7897.

[33] Y. Sakatani, D. Grosso, L. Nicole, C. Boissiere, G.J.D.A.A. Soler-Illia, C. Sanchez, Optimised photocatalytic activity of grid-like mesoporous TiO<sub>2</sub> films: effect of crystallinity, pore size distribution, and pore accessibility, *J. Mater. Chem.* 16 (2006) 77–82.

[34] M.A. Carreon, S.Y. Choi, M. Mamak, N. Chopra, G.A. Ozin, Pore architecture affects photocatalytic activity of periodic mesoporous nanocrystalline anatase thin films, *J. Mater. Chem.* 17 (2007) 82–89.

[35] J.C. Yu, X. Wang, X. Fu, Pore-wall chemistry and photocatalytic activity

- of mesoporous titania molecular sieve films, *Chem. Mater.* 16 (2004) 1523–1530.
- [36] Y. Sakatani, D. Grosso, L. Nicole, C. Boissiere, G.J.D.A.A. Soler-Illia, C. Sanchez, Optimised photocatalytic activity of grid-like mesoporous TiO<sub>2</sub> films: effect of crystallinity, pore size distribution, and pore accessibility, *J. Mater. Chem.* 16 (2006) 77–82.
- [37] P. Hartmann, D.K. Lee, B.M. Smarsly, J. Janek, Mesoporous TiO<sub>2</sub>: Comparison of classical sol–gel and nanoparticle based photoelectrodes for the water splitting reaction, *ACS Nano* 4 (2010) 3147–3154.
- [38] M.A. Carreon, S.Y. Choi, M. Mamak, N. Chopra, G.A. Ozin, Pore architecture affects photocatalytic activity of periodic mesoporous nanocrystalline anatase thin films, *J. Mater. Chem.* 17 (2007) 82–89.
- [39] M. Wark, J. Tschirch, O. Bartels, D. Bahnemann, J. Rathousk, Photocatalytic activity of hydrophobized mesoporous thin films of TiO<sub>2</sub>, *Microporous Mesoporous Mater.* 84 (2005) 247–253.
- [40] F. Bosc, A. Ayrat, P.A. Albouy, L. Datas, C. Guizard, Mesostructure of anatase thin films prepared by mesophase templating, *Chem. Mater.* 16 (2004) 2208–2214
- [41] Y. Sakatani, D. Grosso, L. Nicole, C. Boissiere, G.J.D.A.A. Soler-Illia, C. Sanchez, Optimised photocatalytic activity of grid-like mesoporous TiO<sub>2</sub> films: effect of crystallinity, pore size distribution, and pore accessibility, *J. Mater. Chem.* 16 (2006) 77–82.
- [42] J.C. Yu, X. Wang, X. Fu, Pore-wall chemistry and photocatalytic activity of mesoporous titania molecular sieve films, *Chem. Mater.* 16 (2004) 1523–1530.
- [43] J.H. Pan, W.I. Lee, Preparation of highly ordered cubic mesoporous WO<sub>3</sub>/TiO<sub>2</sub> films and their photocatalytic properties, *Chem. Mater.* 18 (2006) 847–853

- [44] J.H. Pan, S.Y. Chai, W.I. Lee, Photocatalytic properties of mesoporous TiO<sub>2</sub> films derived from evaporation-induced self-assembly method, *Mater. Sci. Forum* 510–511 (2006) 58–61.
- [45] H. Oveisi, S. Rahighi, X. Jiang, Y. Nemoto, A. Beitollahi, S. Wakatsuki, Y. Yamauchi, Unusual antibacterial property of mesoporous titania films: Drastic improvement by controlling surface area and crystallinity, *Chem. Asian J.*
- [46] Y.J. Kim, M.H. Lee, H.J. Kim, G. Lim, Y.S. Choi, N.G. Park, K. Kim, W.I. Lee, Formation of highly efficient dye-sensitized solar cells by hierarchical pore generation with nanoporous TiO<sub>2</sub> spheres, *Adv. Mater.* 21 (2009) 3668–3673. (2010) 1978–1983.
- [47] K. Hou, B. Tian, F. Li, Z. Bian, D. Zhao, C. Huang, *J. Mater. Chem.* 15 (2005) 2414.
- [48] M. Zukalová, A. Zukal, L. Kavan, M.K. Nazeeruddin, P. Liska, M. Grätzel, *Nano Lett.* 5(2005) 1789.
- [49] K. Hou, B. Tian, F. Li, Z. Bian, D. Zhao, C. Huang, *J. Mater. Chem.* 15 (2005) 2414.
- [50] M. Zukalová, A. Zukal, L. Kavan, M.K. Nazeeruddin, P. Liska, M. Grätzel, *Nano Lett.* 5(2005) 1789.
- [51] Yu Zhang, Zhibin Xie, John Wang, *Thin Solid Films* 518 (2010) e34–e37
- [52] Y.Q. Wang, S.G. Chen, X.H. Tang, O. Palchik, A. Zaban, Y. Koltypin, A. Gedanken, *J. Mater. Chem.* 11 (2001) 521.
- [53] D. Grosso, F. Cagnol, G.J. de A.A. Soler-Illia, E.L. Crépaldi, H. Amenitsch, A. Brunet-Bruneau, A. Bourgeois, C. Sanchez, *Adv. Funct. Mater.* 14 (2004) 309
- [54] Luke B. Roberson, Mark A. Poggi, Janusz Kowalik, Greg P. Smestad, Lawrence A. Bottomley, Laren M. Tolbert *Coordination Chemistry Reviews* 248 (2004) 1491–1499

- [55] Jia Hong Pana, X.S. Zhaoa,\* Wan In Leeb,\* *Chemical Engineering Journal* 170 (2011) 363–380
- [56] U. Bach, D. Lupo, P. Comte, J.E. Moser, F. Weissörtel, J. Salbeck, H. Spreitzer, M. Grätzel, *Nature* 395 (1998) 544.
- [57] A. Hagfeldt, M. Grätzel, *Acc. Chem. Res.* 33 (2000) 269–277.
- [58] S.D. Burnside, V. Shklover, Ch. Barbé, P. Comte, F. Arendse, K. Brooks, M. Grätzel, *Chem. Mater.* 10 (1998) 2419.
- [59] V. Shklover, Unpublished HRTEM results.
- [60] U. Bach, Y. Tachibana, J.-E. Moser, S.A. Haque, J.R. Durrant, M. Grätzel, D.R. Klug, *J. Am. Chem. Soc.* 121 (32) (1999) 7445–7446.
- [61] J. Fang, L. Su, J. Wu, Y. Shen, Z. Lu, *N. J. Chem.* 270 (1997) 145.
- [62] R. Plass, S. Pelet, J. Krüger, M. Grätzel, U. Bach, *J. Phys. Chem. B* 106 (2002) 7578–7580.
- [63] Nelson, *J. Phys. Rev. B* 59 (1999) 15374–15380.
- [64] J. Van de Lagemaat, N.G. Park, A.J. Frank, *J. Phys. Chem. B* 104 (2000) 2044.
- [65] L. Dloczik, O. Ileperuma, I. Lauermann, L.M. Peter, E.A. Ponomarev, G. Redmond, N.J. Shaw, I. Uhlendorf, *J. Phys. Chem. B* 101 (1997) 10281.
- [66] S. Nakade, Y. Saito, W. Kubo, T. Kanzaki, T. Kitamura, Y. Wada, S. Yanagida, *Electrochem. Commun.* 5 (2003) 804.
- [67] M. Adachi, Y. Murata, I. Okada, S. Yoshikawa, *J. Electrochem. Soc.* 15 (2003) G488–G493.
- [68] Z.R. Tian, J.A. Voigt, J. Liu, B. Mckenzie, H. Xu, *J. Am. Chem. Soc.* 125 (41) (2003) 12384–12385.
- [69] W.U. Huynh, J.J. Dittmer, A.P. Alivisatos, *Science* 295 (2002) 242.
- [70] V. Shklover, Y.E. Ovchinnikov, L.S. Braginsky, S.M. Zakeeruddin, M. Grätzel, *Chem. Mater.* 10 (1998) 2533.
- [71] Y Zhang, Z B Xie and J Wang1 *Nanotechnology* 20 (2009) 505602 (9pp)

[72] Khalil Ebrahim Jasim, – University of Bahrain, DSSC-Working Principles, Challenges and Opportunities.

[73] Jia Hong Pan, X.S. Rao, W In Lee, Chemical Engineering Journal, [www.elsevier.com/locate/cej](http://www.elsevier.com/locate/cej), 1385-8947/\$